

Journal: ACP

Title: Aliphatic Carbonyl Compounds (C8–C26) in Wintertime Atmospheric Aerosol in London, UK

Author(s): Ruihe Lyu et al.

MS No.: acp-2018-769

RESPONSE TO CO-EDITOR

Sect 3.3: The $\log(K_p)$ vs $\log(VP_t)$ results should be discussed in more detail. For instance, according to Pankow (1994) the slope of this plot should be about -1. For the alkanals, the slope is sometimes positive. Please discuss. Since samples were collected for 24 h, how was the temperature determined? How does the diurnal evolution of temperature affect the results?

RESPONSE: New text has been added as follows:

According to theory, the gradient of the plot of $\log K_p$ versus $\log (VP_t)$ should be -1 (Pankow, 1994). However, many measurement datasets for a number of semi-volatile compound groups including n-alkanes (Cincinelli et al., 2007; Karanasiou et al., 2007; Mandalakis et al., 2002) and PAH (Callen et al., 2008; Wang et al., 2011; Ma et al., 2011; Mandalakis et al., 2002) show a range of values of gradient, often around -0.5, but ranging to below -1, and in some cases positive. Callen et al., (2008) discuss the reasons for deviation from a value of -1, which include a lack of equilibrium, absorption into the organic matter (shallow than -0.6), adsorption processes (steeper than -1), and the averaging of conditions across a range of temperatures during a sampling period.

Our data for alkan-2-ones show high r^2 values and values of gradient (m) in the range of the literature for other groups of semi-volatile compounds. Average gradients at the four sites ranged from -0.46 to -0.26. The alkan-3-ones show generally considerably lower values of r^2 and average values of gradient at the four sites of -0.43 to -0.23. This poorer correlation could be the result of lower analytical precision. The n-alkanals show still lower values of r^2 , and more variable and shallower values of slope. Mean slopes for the four sites ranged from -0.23 to -0.16. There were no positive daily values. The lower r^2 may be a result of disequilibrium for the alkanals which are dominated by primary emissions, and are also more reactive. It might also reflect a role for aqueous aerosol as an absorbing medium for these compounds containing a significant polar moiety, which would lead to deviations from the Pankow (1994) theory, and more variable behaviour as the availability of aqueous particles into which to partition would depend upon relative humidity, which is itself highly variable.

Samples were collected over 24-hour periods and hence the diurnal variation of temperature may be relevant. Temperature data were taken from Heathrow Airport to the west of London and did not show large diurnal fluctuations, so this should not be a major factor. The average diurnal temperature range based upon hourly data was 6.9°C.

Table 2: The % of n-alkanals in the particle phase is surprisingly high for the low C number species. Please comment on this.

RESPONSE: We have re-evaluated our recovery data and have excluded vapour phase compounds of C₈ and C₉ from the data analysis as these were not collected quantitatively.

Minor:

Abstract: Please make it clear that both gas- and condensed-phase measurements were made as part of this work.

RESPONSE: This has been accomplished.

Sect 2.3: Please also include limit of detections for the compounds as this becomes a point later on in the manuscript. Also, please add information on breakthrough that was included in the response to Referee 2. What exactly is meant by "minimal breakthrough for alkanes >= C11"? Was loss of gas-phase compounds to the filters investigated?

RESPONSE: Limits of detection have been added to the Supplementary Information. Six tests of vapour breakthrough were conducted with two adsorption tubes in series. Recovery was good for all compounds $\geq C_{11}$, and for C_{10} was 85% for all three compound groups. This is now clarified in the text. No tests of vapour uptake to the filters were conducted, but as PTFE filters were used uptake is not to be expected (unlike quartz).

Line 208: The time series is Figure 3 not 2. Please ensure that all figures are referenced in order and that the correct figure is referenced in the text throughout the manuscript.

RESPONSE: This has been corrected.

Line 214-216: These references did not specifically identify the position of the carbonyl group. Please revise.

RESPONSE: Revised to clarify the point.

Line 228-229: Wouldn't this be independent of NO concentration if the issue is reaction with O₂ vs isomerization?

RESPONSE: There was a typographic error which has been corrected. The role of NO is in converting the alkylperoxy radical to an alkoxy radical which isomerises, rather than reacting with O₂.

Line 252-253: I am not convinced that the difference in concentration is a "clear indication of road traffic." I would expect that the urban measurements would also be influenced by traffic. More details regarding the previous work (site locations, temperature, time of year, etc.) needs to be provided if this sentence remains.

RESPONSE: An explanatory sentence has been added as follows:

Earlier work has clearly demonstrated a substantial elevation in traffic-generated pollutants at the Marylebone Road site, relative to background sites within London (Harrison and Beddows, 2017).

Line 261: Please define Cmax the first time it is used.

RESPONSE: This has been amended.

Line 286: CPI is used before it is defined. Please correct this.

RESPONSE: This has been amended.

Line 347-348: Please be more explicit about what is meant by "significant particulate fraction" and "low MW."

RESPONSE: This refers to a particulate fraction >60% and n-alkanes of C₁₄-C₁₈, and the text has been amended.

Line 355-357: For alkanes of this size, isomerization in the gas-phase dominates over fragmentation. As such I would think that decomposition products would likely be multifunctional. I would also expect that aldehydes would be preferentially formed as a result of fragmentation. Please clarify how this could occur.
RESPONSE: The word "likely" has been changed to "possible", and the following has been added to the sentence:

"....although fragmentation reactions would result mainly in the formation of alkanals, and are less likely to occur than isomerisation leading mostly to multifunctional products.".

Line 365-366: Please clarify that homogeneous means gas-phase.

RESPONSE: This has been clarified.

Table S4 I see data for only RU and WM sites, however, the caption says that it includes data for El and MR site. Please fix.

RESPONSE: The full dataset for all sites is now included.

Lines 582-588: This seems better suited for Sect. 3.3 then for the conclusions.

RESPONSE: This is within the new text in Section 3.3, and has therefore been shortened to a summary within the Conclusions.

1

2

3 **Aliphatic Carbonyl Compounds (C₈-C₂₆) in Wintertime**
4 **Atmospheric Aerosol in London, UK**

5

6 **Ruihe Lyu^{1,2}, Mohammed Salim Alam¹, Christopher Stark¹**

7 **Ruixin Xu¹, Zongbo Shi¹, Yinchang Feng² and Roy M. Harrison^{†*1}**

8

9 **¹ Division of Environmental Health and Risk Management**

10 **School of Geography, Earth and Environmental Sciences, University of**

11 **Birmingham Edgbaston, Birmingham B15 2TT, UK**

12

13 **² State Environmental Protection Key Laboratory of Urban Ambient Air**

14 **Particulate Matter Pollution Prevention and Control, College of Environmental**
15 **Science and Engineering**

16 **Nankai University, Tianjin 300350, China**

17

18

19

20 **† Also at: Department of Environmental Sciences / Centre of Excellence in Environmental**
21 **Studies, King Abdulaziz University, PO Box 80203, Jeddah, 21589, Saudi Arabia.**

22

23 **Corresponding authors:**

24 **E-mail: r.m.harrison@bham.ac.uk (Roy M. Harrison)**

25

26

27 **ABSTRACT**

28 Three groups of aliphatic carbonyl compounds, the n-alkanals (C_8-C_{20}), n-alkan-2-ones (C_8-C_{26}) and
29 n-alkan-3-ones (C_8-C_{19}) were measured in both particulate and vapour phases in air samples collected
30 in London from January-April 2017. Four sites were sampled including two roof-top background
31 sites, one ground-level urban background site and a street canyon location on Marylebone Road in
32 central London. The n-alkanals showed the highest concentrations followed by the n-alkan-2-ones
33 and the n-alkan-3-ones, the latter having appreciably lower concentrations. It seems likely that all
34 compound groups have both primary and secondary sources and these are considered in the light of
35 published laboratory work on the oxidation products of high molecular weight n-alkanes. All
36 compound groups show relatively low correlation with black carbon and NOx in the background air
37 of London, but in street canyon air heavily impacted by vehicle emissions, stronger correlations
38 emerge especially for the n-alkanals. It appears that vehicle exhaust is likely to be a major contributor
39 for concentrations of the n-alkanals whereas it is a much smaller contributor to the n-alkan-2-ones
40 and n-alkan-3-ones. Other primary sources such as cooking or wood burning may be contributors for
41 the ketones but were not directly evaluated. It seems likely that there is also a significant contribution
42 from photo-oxidation of n-alkanes and this would be consistent with the much higher abundance of
43 the n-alkan-2-ones relative to the n-alkan-3-ones if the formation mechanism were to be through
44 oxidation of condensed phase alkanes. Vapour-particle partitioning fitted the Pankow model well for
45 the n-alkan-2-ones but less well for the other compound groups, although somewhat stronger
46 relationships were seen at the Marylebone Road site than at the background sites. The former
47 observation gives support to the n-alkane-2-ones being a predominantly secondary product, whereas
48 primary sources of the other groups are more prominent.

49 **Keywords:** Carbonyl compounds; n-alkanals; n-alkan-2-ones; n-alkan-3-ones; organic aerosol;
50 partitioning;

51 **1. INTRODUCTION**

52 Carbonyl compounds are classified as polar organic compounds, constituting a portion of the
53 oxygenated organic compounds in atmospheric particulate matter (PM). Aliphatic carbonyl
54 compounds are directly emitted into the atmosphere from primary biogenic and anthropogenic
55 sources (Schauer et al., 2001, 2002a, b), as well as being secondary products of atmospheric
56 oxidation of hydrocarbons (Chacon-Madrid et al., 2010; Zhang et al., 2015; Han et al., 2016).

57

58 The most abundant atmospheric carbonyls are methanal (formaldehyde) and ethanal (acetaldehyde),
59 and many studies have described their emission sources and chemical formation in urban and rural
60 samples (Duan et al., 2016). Long-chain aliphatic carbonyl compounds have been identified in PM
61 and reported in few published papers (Gogou et al., 1996; Andreou and Rapsomanikis, 2009), and
62 these compounds are considered to be formed from atmospheric oxidation processes affecting
63 biogenic emissions of alkanes. Anthropogenic activity is also considered to be a significant
64 contributor to the aliphatic carbonyls. Appreciable concentrations of aliphatic carbonyl compounds
65 have been identified in emissions from road vehicles (Schauer et al., 1999a; 2002b), coal combustion
66 (Oros and Simoneit, 2000), wood burning (Rogge et al., 1998) and cooking processes (Zhao et al.,
67 2007a,b), spanning a wide range of molecular weights. Furthermore, chamber studies (Chacon-
68 Madrid and Donahue, 2011; Algrim and Ziemann, 2016) have demonstrated that the aliphatic
69 carbonyl compounds are very important precursors of secondary organic aerosol (SOA) when they
70 react with OH radicals in the presence of NO_x.

71

72 The oxidation of n-alkanes by hydroxyl radical is considered to be an important source of aliphatic
73 carbonyl compounds. It was believed that the n-alkanals with carbon atoms numbering less than 20
74 indicate oxidation of alkanes, whereas the higher compounds were usually considered to be of direct
75 biogenic origin (Rogge et al., 1998). The homologues and isomers of n-alkanals and n-alkanones have
76 been identified as OH oxidation products of n-alkanes in many chamber and flow tube studies (Zhang
77 et al., 2015; Schilling Fahnstock et al., 2015; Ruehl et al., 2013; Yee et al., 2012), although not all
78 studies identified the position of the carbonyl group. The commonly accepted oxidation pathways of
79 n-alkanes generally divide into functionalization and fragmentation. Functionalization occurs when
80 an oxygenated functional group ($-\text{ONO}_2$, $-\text{OH}$, $-\text{C=O}$, $-\text{C}(\text{O})\text{O}-$ and $-\text{OOH}$) is added to a molecule,
81 leaving the carbon skeleton intact. Alternatively, fragmentation involves C–C bond cleavage and
82 produces two oxidation products with smaller carbon numbers than the reactant. The chamber studies
83 of dodecane oxidation include observations of aldehydes and ketones as oxidation products (Schilling
84 Fahnstock et al., 2015; Yee et al., 2012).

85

86 In London, with a high population density and a large number of diesel engine vehicles, the aliphatic
87 hydrocarbons constitute an important fraction of ambient aerosols. Anthropogenic activities and
88 secondary formation contribute to the emission and production of carbonyl compounds within the
89 city. The objectives of the present study were the identification and quantification of aliphatic
90 carbonyl compounds in particle and vapour samples collected in London from January to April 2017.
91 This work has aided an understanding of the concentrations and secondary formation of carbonyls in
92 the London atmosphere. Spatial and temporal variations of the studied carbonyl compounds were
93 assessed and used to infer sources. One of the main objectives was to provide gas/particle partitioning

94 coefficients of identified carbonyls under realistic conditions. Diagnostic criteria were used to
95 estimate the sources of identifiable atmospheric carbonyl compounds. Additionally, for the first time,
96 concentrations of particulate and gaseous n-alkan-3-ones are reported.

97

98 **2. MATERIALS AND METHODS**

99 **2.1 Sampling Method and Site Characteristics**

100 Three sampling campaigns were carried out between 23 January and 18 April 2017 at four sampling
101 sites (Figure 1) in London. The first campaign used two sampling sites, one located on the roof of a
102 building (15 m above ground) of the Regent's University (51°31'N, -0°9'W), hereafter referred to as
103 RU, sampled from 23 January 2017 to 19 February 2017, the other located on the roof (20 m above
104 ground) of a building which belongs to the University of Westminster on the southern side of
105 Marylebone Road (hereafter referred to as WM), sampled from 24 January 2017 to 20 February 2017.

106 The third sampling site was located at ground level at Eltham (51°27'N, 0°4'E), hereafter referred to
107 as EL, sampled from 23 February 2017 to 21 March 2017, which is located in suburban south London,
108 and the fourth sampling site was located at ground level on the southern side of Marylebone Road
109 (51°31'N, -0°9'W), hereafter referred to as MR, sampled from 22 March 2017 to 18 April 2017.

110 Marylebone Road is in London's commercial centre, and is an important thoroughfare carrying 80-
111 90,000 vehicles per day through central London. The Regent's University site is within Regent's
112 Park to the north of Marylebone Road. The Eltham site is in a typical residential neighbourhood, 22
113 km from the MR site. Earlier work at the Marylebone Road and a separate Regent's Park site is
114 described by Harrison et al. (2012).

115 The particle samples were collected on polypropylene backed PTFE filters (47 mm, Whatman) which
116 preceded stainless steel sorbent tubes packed with 1cm quartz wool, 300 mg Carbograph 2TD 40/60
117 (Markes International, Llantrisant, UK) and sealed with stainless-steel caps before and after sampling.
118 Sampling took place for sequential 24-hour periods at a flow rate of 1.5 L min^{-1} using an in-house
119 developed automated sampler. Field blank filters and sorbent tubes were prepared for each site, and
120 recovery efficiencies were evaluated. Adsorption tube breakthrough was tested in the field with six
121 replicates of two tubes in series and for compounds of $\geq \text{C}_{11}$ recovery exceeded 95% on the first tube.
122 It was 85% for the C_{10} compounds, and lower for C_9 and C_8 for which data are not reported. After
123 the sampling, each filter was placed in a clean sealed petri dish, wrapped in aluminium foil and stored
124 in the freezer at -18°C prior to analysis. Black carbon (BC) was simultaneously monitored during the
125 sampling period at RU and WM sites using an aethalometer (Model AE22, Magee Science).
126 Measurements of BC and NO_x at MR and NO_x at EL were provided by the national network sites of
127 Marylebone Road, and Eltham (<https://uk-air.defra.gov.uk/>).

128

129 2.2 Analytical Instrumentation

130 The particle samples were analyzed using a 2D gas chromatograph (GC, 7890A, Agilent
131 Technologies, Wilmington, DE, USA) equipped with a Zoex ZX2 cryogenic modulator (Houston,
132 TX, USA). The first dimension was equipped with a SGE DBX5, non-polar capillary column (30.0
133 m, 0.25 mm ID, 0.25 mm – 5.00% phenyl polysilphenylene-siloxane), and the second-dimension
134 column equipped with a SGE DBX50 (4.00 m, 0.10 mm ID, 0.10 mm – 50.0% phenyl
135 polysilphenylene-siloxane). The $\text{GC} \times \text{GC}$ was interfaced with a Bench-ToF-Select, time-of-flight
136 mass spectrometer (ToF-MS, Markes International, Llantrisant, UK). The acquisition speed was 50.0

137 Hz with a mass resolution of >1200 fwhm at 70.0 eV and the mass range was 35.0 to 600 m/z. All
138 data produced were processed using GC Image v2.5 (Zoex Corporation, Houston, US).

139

140 **2.3 Analysis of Samples**

141 Standards used in these experiments included 19 alkanes, C₈ to C₂₆ (Sigma-Aldrich, UK, purity
142 >99.2%); 12 n-aldehydes, C₈ to C₁₃ (Sigma-Aldrich, UK, purity ≥95.0%), C₁₄ to C₁₈ (Tokyo
143 Chemical Industry UK Ltd, purity >95.0%); and 10 2-ketones, C₈ to C₁₃ and C₁₅ to C₁₈ (Sigma-
144 Aldrich, UK, purity ≥98.0%) and C₁₄ (Tokyo Chemical Industry UK Ltd, purity 97.0%).

145

146 The filters were spiked with 30.0 µL of 30.0 µg mL⁻¹ deuterated internal standards (dodecane-d₂₆,
147 pentadecane-d₃₂, eicosane-d₄₂, pentacosane-d₅₂, triacontane-d₆₂, butylbenzene-d₁₄, nonylbenzene-
148 2,3,4,5,6-d₅, biphenyl-d₁₀, p-terphenyl-d₁₄; Sigma-Aldrich, UK) for quantification and then
149 immersed in dichloromethane (DCM), and ultra-sonicated for 20.0 min at 20.0°C. The extract was
150 filtered using a clean glass pipette column packed with glass wool and anhydrous Na₂SO₄, and
151 concentrated to 50.0 µL under a gentle flow of nitrogen for analysis using GC × GC-ToF-MS. 1 µL
152 of the extracted sample was injected in a split ratio 100:1 at 300°C. The initial temperature of the
153 primary oven (80.0°C) was held for 2.0 min and then increased at 2.0 °C min⁻¹ to 210°C, followed by
154 1.5 °C min⁻¹ to 325 °C. The initial temperature of the secondary oven (120°C) was held for 2.0 min
155 and then increased at 3.0°C min⁻¹ to 200°C, followed by 2.00°C min⁻¹ to 300°C and a final increase
156 of 1.0°C min⁻¹ to 330 °C to ensure all species passed through the column. The transfer line
157 temperature was 330 °C and the ion source temperature was 280°C. Helium was used as the carrier

158 gas at a constant flow rate of 1.0 mL min⁻¹. Further details of the instrumentation and data processing
159 methods is given by Alam et al. (2016a,b).

160

161 The sorbent tubes were analyzed by an injection port thermal desorption unit (Unity 2, Markes
162 International, Llantrisant, UK) and subsequently analyzed using GC × GC-ToF-MS. Briefly, the
163 tubes were spiked with 1 ng of deuterated internal standard for quantification and desorbed onto the
164 cold trap at 350°C for 15.0 min (trap held at 20.0°C). The trap was then purged onto the column in
165 a split ratio of 100:1 at 350°C and held for 4.0 min. The initial temperature of the primary oven
166 (90.0°C) was held for 2.0 min and then increased to 2.0°C min⁻¹ to 240°C, followed by 3.0°C min⁻¹
167 to 310°C and held for 5.0 min. The initial temperature of the secondary oven (40.0°C) was held for
168 2.0 min and then increased at 3.0°C min⁻¹ to 250°C, followed by an increase of 1.5°C min⁻¹ to 315°C
169 and held for 5.0 min. Helium was used as carrier gas for the thermally desorbed organic compounds,
170 with a gas flow rate of 1.0 mL min⁻¹.

171

172 *Qualitative analysis*

173 Compound identification was based on the GC×GC-TOFMS spectra library, NIST mass spectral
174 library and in conjunction with authentic standards. Compounds within the homologous series for
175 which standards were not available were identified by comparing their retention time interval between
176 their homologues, and by comparison of mass spectra to the standards for similar compounds within
177 the series, by comparison to the NIST mass spectral library and by the analysis of fragmentation
178 patterns.

179 *Quantitative analysis*

180 An internal standard solution (outlined above) was added to the samples to extract prior to
181 instrumental analysis. Five internal standards (pentadecane-d₃₂, eicosane-d₄₂, pentacosane-d₅₂,
182 triacontane-d₆₂, nonylbenzene-2,3,4,5,6-d₅) were used in the calculation of carbonyl compound
183 concentrations.

184

185 The quantification for alkanes, aldehydes and 2-ketones was performed by the linear regression
186 method using seven-point calibration curves (0.05, 0.10, 0.25, 0.50, 1.00, 2.00, 3.00 ng μL^{-1})
187 established between the authentic standards/internal standard concentration ratios and the
188 corresponding peak area ratios. The calibration curves for all target compounds were highly linear
189 ($r^2 > 0.99$, from 0.990 to 0.997), demonstrating the consistency and reproducibility of this method.

190 Limits of detection for individual compounds were typically in the range 0.04–0.12 ng m^{-3} . 3-ketones
191 were quantified using the calibration curves for 2-ketones. This applicability of quantification of
192 individual compounds using isomers of the same compound functionality (which have authentic
193 standards) has been discussed elsewhere and has a reported uncertainty of 24% (Alam et al., 2018).
194 Alkan-2-ones and alkan-3-ones were not well separated by the chromatography. These were separated
195 manually using the peak cutting tool, attributing fragments at m/z 58 and 71 to 2-ketones and m/z 72
196 and 85 to 3-ketones.

197

198 Field and laboratory blanks were routinely analysed to evaluate analytical bias and precision. Blank
199 levels of individual analytes were normally very low ~~and in most cases not detectable~~. Recovery
200 efficiencies were determined by analyzing the blank samples spiked with standard compounds. Mean

201 recoveries ranged between 78.0 and 102%. All quantities reported here have been corrected according
202 to their recovery efficiencies. Detection limits are reported in Table S1.

203

204 **3. RESULTS AND DISCUSSION**

205 **3.1 Mass Concentration of Particle-Bound Carbonyl Compounds**

206 The study of temporal and spatial variations of air pollutants can provide valuable information about
207 their sources and atmospheric processing. The time series of particle-bound n-alkanals, n-alkan-2-
208 ones, and n-alkan-3-ones are plotted in Figure 2. It is clear that the concentrations of n-alkanals varied
209 substantially with date, and were always higher than n-alkanones at four sites. It is also clear from
210 Figure 3 that concentrations were broadly similar at the background sites, RU, WM and EL, but are
211 elevated, especially for the n-alkanals, at MR. This is strongly indicative of a road traffic source.

212

213 Carbonyls including n-alkan-2-one and n-alkan-3-onen-alkanone homologues could result as
214 fragmentation products from larger alkane precursors during gas-phase oxidation (Yee et al., 2012;
215 Schilling Fahnstock et al., 2015) or as functionalized products from heterogeneous oxidation of
216 particle-bound alkanes (Ruehl et al., 2013; Zhang et al., 2015). While carbonyl compounds are
217 expected to be amongst first generation oxidation products of alkanes, product yields are not well
218 known, and are highly dependent upon the chemical environment in which oxidation occurs. Yee
219 et al. (2012) show substantial yields of mono-carbonyl product, the position of substitution undefined,
220 in the low-NO_x oxidation of n-dodecane. Ruehl et al. (2013) report the production of 2- through 14-
221 octacosanone from the oxidation of octacosane, giving relative, but not absolute yields. Schilling

222 Fahnestock et al. (2014) report oxidation products of dodecane formed in both low-NO and high NO
223 environments (<d.1 and NO = 97.5 ppb respectively). A singly substituted unfragmented ketone
224 product is reported only from the low-NO oxidation, and in relatively low yield amongst many
225 products. Lim and Ziemann (2009) propose a reaction scheme for the OH-initiated oxidation of
226 alkanes in the presence of NO_x. They express the view that first generation carbonyl formation is
227 negligible at high NO concentrations for linear alkanes with C_n>6 since reactions of an **alkylperoxy**
228 **alkoxy** radical with O₂ are to slow to compete with isomerisation, which leads ultimately to
229 hydroxynitrate and hydroxycarbonyl products. Ziemann (2011) also shows a substantial yield of
230 alkynitrates from OH-initiated oxidation of n-alkanes from C₁₀-C₂₅ in the presence of NO. The NO
231 concentrations in the background air of London are <12 ppb typically (UK-Air, 2018), and hence lie
232 between the low and high NO environments of experiments in the literature, therefore most probably
233 permitting some oxidation to proceed through pathways leading to first generation carbonyl products.

234

235 Figure 3 shows the average total concentrations of particle-bound 1-alkanals, n-alkan-2-ones, and
236 n-alkan-3-ones from January to April at four measurement sites, and the particle and gaseous phase
237 concentrations are detailed in the Table **S1-S2** (Supporting Information). Total n-alkanals was
238 defined as the sum of particle-bound n-alkanals ranging from C₈ to C₂₀. The particulate n-alkanals
239 at the MR site accounted for 75.2% of the measured particle carbonyls with the average total
240 concentration of 682 ng m⁻³, and concentrations at the other sites were 167 ng m⁻³ at EL, 117 ng m⁻³
241 at WM and 82.6 ng m⁻³ at RU, accounting for 57.0%, 57.9% and 56.3% of the measured particulate
242 carbonyls, respectively. The n-alkanals identified in this study differed substantially from those
243 previously reported in samples collected from Crete (Gogou et al., 1996) and Athens (Andreou and

244 Rapsomanikis, 2009) in Greece. The n-alkanals from London presented narrower ranges of carbon
245 numbers and a higher concentration than rural and urban samples from Crete. The concentrations of
246 n-alkanal homologues (C₈-C₂₀) ranged from 5.50 to 141 ng m⁻³ (average 52.0 ng m⁻³) at MR which
247 were far higher than 1.48-28.6 ng m⁻³ (average 6.44 ng m⁻³) at RU, 1.42-50.3 ng m⁻³ (average 9.03
248 ng m⁻³) at WM and 3.29-53.0 ng m⁻³ (average 13.0 ng m⁻³) at EL (Table S1), unlike Crete where the
249 concentrations were 0.9-3.7 ng m⁻³ in rural (C₁₅-C₃₀) and 5.4-6.7 ng m⁻³ in urban (C₉-C₂₂) samples,
250 and the average concentration of all four sites was much higher than the 0.91 ng m⁻³ measured in
251 Athens (Andreou and Rapsomanikis, 2009) (C₁₃-C₂₀). This is a clear indication of a road traffic,
252 most probably diesel source which is greater in London. Earlier work has clearly demonstrated a
253 substantial elevation in traffic-generated pollutants at the Marylebone Road site, relative to
254 background sites within London (Harrison and Beddows, 2017).

255

256 As part of the CARBOSOL project (Oliveira et al., 2007), air samples were collected in summer and
257 winter at six rural sites across Europe. The particulate n-alkanals ranged from C₁₁ to C₃₀ with average
258 total concentrations between 1.0 ng m⁻³ and 19.0 ng m⁻³, with higher concentrations in summer than
259 winter at all but one site. Maximum concentrations at all sites were in compounds >C₂₂ indicating a
260 source from leaf surface abrasion products and biomass burning (Simoneit et al., 1967; Gogou et al.,
261 1996). This far exceeds the C_{max} (carbon number of the most abundant homologue) values seen in
262 the particulate fraction at our sites.

263

264 The n-alkan-2-one homologues measured in London ranged from C₈ to C₂₆, and the average total
265 particulate fraction concentration was 58.5 ng m⁻³ at RU, 75.1 ng m⁻³ at WM, 112 ng m⁻³ at EL and

266 186 ng m⁻³ at MR, approximately accounting for 39.9% (RU), 37.0% (WM), 38.1% (EL) and 20.5%
267 (MR) of the total particulate carbonyls, respectively (Figure 3). The published data from Greece
268 indicated that the concentrations of n-alkan-2-ones were independent of the seasons, and an average
269 of 5.40 ng m⁻³ (C₁₃-C₂₉) was measured in August and 5.44 ng m⁻³ in March at Athinas St, but 12.88
270 ng m⁻³ was measured in March at the elevated (20 m) AEDA site in Athens (Gogou et al., 1996).
271 Concentrations in Crete for alkan-2-ones (C₁₀-C₃₁) were 0.4-2.1 ng m⁻³ at the rural site and 1.9-2.6
272 ng m⁻³ at the urban site (Andreou and Rapsomanikis, 2009). The CARBOSOL project also
273 determined concentrations of n-alkan-2-ones, between C₁₄ and C₃₁ with a C_{max} at C₂₈ or C₂₉ at all
274 but one site. Average concentrations ranged from 0.15 ng m⁻³ (C₁₇₋₂₉) to 3.35 (C_{14-C₃₁}), very much
275 below the concentrations at our London sampling site. Cheng et al. (2006) measured concentrations
276 of n-alkan-2-ones in the Lower Fraser Valley, Canada, in PM_{2.5}. Samples collected in a road tunnel
277 showed the highest concentrations, total 1.8-12.6 ng m⁻³ for C₁₀-C₃₁, and were higher in daytime
278 than nighttime. Concentrations at a forest site were 1.1-7.2 ng m⁻³ without a diurnal pattern. Values
279 of C_{max} ranged from C₁₆₋₁₇ at the road tunnel to C₂₇ (secondary maximum) at the forest site. Values
280 of CPI ([Carbon Preference Index, defined in Section 3.2.1](#)) averaged across sites from 1.00 to 1.34,
281 giving little evidence for a substantial biogenic input from higher plant waxes. These data clearly
282 suggest a road traffic source in London, but less influential than for the n-alkanals for which the
283 increment at the roadside MR site is much greater.

284

285 The n-alkan-3-one homologues identified in the samples ranged from C₈ to C₁₉, and the average of
286 individual compound concentrations was 0.52 ng m⁻³ at RU, 0.94 ng m⁻³ at WM, 1.37 ng m⁻³ at EL
287 and 3.34 ng m⁻³ at MR. The concentrations of n-alkan-3-ones at the four sites were lower than the n-

288 alkanals and n-alkan-2-ones, and MR had the highest average total mass concentrations 39.4 ng m^{-3}
289, followed by 14.3 ng m^{-3} at EL, 10.4 ng m^{-3} at WM and 5.65 ng m^{-3} at RU, respectively.

290

291 The isomeric carbonyls formed via OH-initiated heterogeneous reactions of n-octacosane (C_{28})
292 exhibit a pronounced preference at the 2-position of the molecule chain (Ruehl et al., 2013). The n-
293 octacosan-2-ones have the highest relative yield (1.00), followed by n-octacosan-3-ones (0.50), while
294 other isomeric carbonyl yields were lower than 0.20. The same results were found in the subsequent
295 chamber studies of n-alkanes (Zhang et al., 2015) (C_{20} , C_{22} , C_{24} but not C_{18}). The main probable
296 reason was that a large fraction of C_{18} evaporated into the gas phase, and OH oxidation happened in
297 the gas phase (homogeneous reaction). This may be supported by the evidence from previous studies
298 (Kwok and Atkinson, 1995; Ruehl et al., 2013), which found that the isomeric distribution of
299 oxidation products of n-alkanes depends upon whether the reaction occurs in the gas phase or at the
300 particle surface (Kwok and Atkinson, 1995; Ruehl et al., 2013). The homogeneous gas-phase
301 oxidation occurs fast, and H-abstraction by OH radicals occurs at all carbon sites. The fractions of
302 the OH radical reaction by H atom abstraction from n-decane at the 1-, 2-, 3-, 4- and 5-positions are
303 3.10%, 20.7%, 25.4%, 25.4%, and 25.4%, respectively, and the products from gas phase
304 (homogeneous) reaction were generally in accord with structure-reactivity relationship (SRR)
305 predictions (Kwok and Atkinson, 1995; Aschmann et al., 2001). Zhang et al. (2015) report on the
306 competition between homogeneous and heterogeneous oxidation of medium to high molecular weight
307 alkanes. They express the view that in the atmosphere, compounds typically classified as semi-
308 volatile evaporate sufficiently rapidly that homogeneous gas phase oxidation is more rapid than
309 oxidation in the condensed phase.

310 During the field experiment, the n-alkanal homologues were abundant in all samples, and this is
311 probably attributable to the primary emission sources, including diesel vehicles (Schauer et al.,
312 1999a), gasoline cars (Schauer et al., 2002b), wood burning (Rogge et al., 1998) and cooking aerosol
313 (Schauer et al., 1999b). Correlations with other largely vehicle-generated pollutants (see later)
314 support this interpretation. The particulate form of the n-alkane homologues (C₁₄-C₃₆) identified in
315 the samples dominated for >C₂₅ and there was a significant particulate fraction (>60%) for all but the
316 low MW n-alkanes (C₁₄-C₁₈) (unpublished data). The H-abstraction by OH radicals may therefore
317 have been dominated by heterogeneous reactions generating the higher concentrations of n-alkan-2-
318 ones than n-alkan-3-ones that were found in all samples. The ratio of n-alkan-2-ones/n-alkan-3-ones
319 (C₁₁-C₁₈) with the same carbon atom number ranged from 2.35-11.3 at four measurement sites.
320 Surprisingly, although the n-alkane (C₁₁-C₁₃) oxidation was expected to be dominated by
321 homogeneous gas phase reactions, the n-alkan-2-one/n-alkan-3-one ratios were still greater than 2.00.
322 The probable reason was that the lower molecular weight n-alkan-2-ones were significantly impacted
323 by primary emission sources such as cooking (Zhao et al., 2007a,b). Another likely possible reason
324 is that the n-alkan-2-one and n-alkan-3-one homologues with lower carbon atom numbers originated
325 in part from the fragmental products of higher n-alkanes (Yee et al., 2012; Schilling Fahnstock et
326 al., 2015), although fragmentation reactions would result mainly in the formation of alkanals, and are
327 less likely to occur than isomerisation leading mostly to multifunctional products.
328
329 The ratios of n-alkan-2-ones/n-alkanes, n-alkan-3-ones/n-alkanes (with same carbon numbers) were
330 calculated and are reported in Table S32. The n-alkan-3-ones with carbon numbers higher than C₂₀
331 were not identified in the samples, indicating that both the gas phase and heterogeneous reactions of

332 higher molecular weight n-alkanes were slow, the former probably due to the low vapour phase
333 presence of n-alkanes. The ratios of n-alkan-3-ones/n-alkanes at four measurement sites gradually
334 increased from C₁₁, and then decreased from C₁₇, while higher ratios of n-alkan-2-ones/n-alkanes were
335 observed in the range from C₁₇ to C₂₂, probably indicating a shift from homogeneous gas phase
336 reactions to heterogeneous reactions with the increase of carbon numbers. The low ratios of n-alkan-
337 2-ones/n-alkanes with carbon numbers from C₂₃ to C₂₆ might be explained by the low diffusion rate
338 from the inner particle to the surface with the increasing carbon number of n-alkanes, even though
339 heterogeneous reactions would be the expected dominant pathway.

340

341 3.2 Sources of Carbonyl Compounds

342 3.2.1 Homologue distribution and carbon preference index (CPI)

343 Figure 4 shows the average concentrations, and molecular distributions of particle-bound carbonyl
344 compounds at the four sites. The values of carbon preference index (CPI) were calculated to estimate
345 the origin of carbonyl compounds, according to Bray and Evans (1961):

346

$$347 CPI = \frac{1}{2} \left(\frac{\sum_4^m C_{2i+1}}{\sum_4^m C_{2i}} + \frac{\sum_4^m C_{2i+1}}{\sum_5^{m+1} C_{2i}} \right)$$

348 For n-alkanals and n-alkan-3-ones (m=9): CPI = $\frac{1}{2} \left(\frac{\sum odd(C_9-C_{19})}{\sum even(C_8-C_{18})} + \frac{\sum odd(C_9-C_{19})}{\sum even(C_{10}-C_{20})} \right)$

349 For n-alkan-2-ones (m=12): CPI = $\frac{1}{2} \left(\frac{\sum odd(C_9-C_{25})}{\sum even(C_8-C_{24})} + \frac{\sum odd(C_9-C_{25})}{\sum even(C_{10}-C_{26})} \right)$

350

351 where i takes values between 4 and m , and 5 and m as in the equation, and

352 $m = 9$ for n-alkanal and n-alkan-3-ones

353 $m = 12$ for n-alkan-2-ones

354 The carbon number of the homologue of highest concentration (C_{max}) can be indicative of the source.

355 Table. 1 presents the CPI and C_{max} of particle-bound carbonyl compounds calculated in the current

356 and other studies. A CPI of ≤ 1 is an indication of an anthropogenic source, while a CPI of 1-5

357 shows a mixture of anthropogenic and biogenic sources and a CPI > 5 suggests a biogenic (plant wax)

358 source.

359

360 The n-alkanes which are potential precursors of the oxygenates described typically showed two C_{max}

361 values, the first at C_{13} (the lowest MW compound measured), and at C_{23} . The CPI values for the

362 n-alkanes were between 0.97-1.02 at the four measurements sites (unpublished data).

363

364 According to the low CPI (0.41-1.07) at the four sites, the n-alkanal homologues with carbon number

365 from C_8 to C_{20} mainly originate from anthropogenic emissions or OH oxidation of fossil-derived

366 hydrocarbons. The particle-bound n-alkanals exhibited a similar distribution of carbon number from

367 January to April at four sites, and they had the same C_{max} at C_8 with concentration 28.6 ng m^{-3} at

368 RU, 50.3 ng m^{-3} at WM, 53.0 ng m^{-3} at EL and 141 ng m^{-3} at MR, respectively. This compound may

369 be a fragmentation product, oxidation product or primary emission. In addition, the distribution of

370 n-alkanals had a second concentration peak at C_{15} (MR) and C_{18} (RU, WM, and EL). The C_{18}

371 compound was observed accounting for the highest percentage of the total mass of n-alkanals in

372 some rural aerosol samples (Gogou et al., 1996) in Crete. Andreou and Rapsomanikis reported the

373 C_{max} as C_{15} or C_{17} in Athens (Andreou and Rapsomanikis, 2009) and attributed this to the oxidation

374 of n-alkanes. However, a C_{max} at C_{26} or C_{28} in urban Crete (Gogou et al., 1996) was observed,
375 suggestive of biogenic input. The homologue distribution and CPI of n-alkanals in this study differed
376 from those previous reports, and demonstrated weak biogenic input and a strong impact of
377 anthropogenic activities in the London samples.

378

379 In this study, n-alkan-2-ones have similar homologue distributions and C_{max} (C_{19} or C_{20}) (Table 2)
380 at RU, WM and EL sites, and the total concentration from C_{16} to C_{23} accounts for 76.0%, 76.1% and
381 68.0% of \sum n-alkan-2-ones, respectively. The CPI values for n-alkan-2-ones ranged from 0.57 to
382 1.23 at the RU, MR and WM sites and were not indicative of major biogenic input, and were
383 considered to mainly originate from anthropogenic activities and OH oxidation of anthropogenic n-
384 alkanes. It is however notable that the CPI values for both the 2-ketones and 3-ketones exceed
385 those for the alkanals (see Table 1), suggesting a contribution from contemporary biogenic sources,
386 possibly wood smoke and cooking. At EL, the CPI of 1.57 is clearly indicative of a biogenic
387 contribution in suburban south London. A difference was observed at the MR site, the n-alkan-2-
388 ones with carbon atoms numbering from C_{12} to C_{18} accounting for 72.0% of \sum n-alkan-2-ones, with
389 the C_{max} being at C_{16} . These data suggest a contribution of primary emissions from traffic at MR,
390 but a dominant background, probably substantially secondary, at the other sites. The C_{max} of n-alkan-
391 3-ones was at C_{16} at the MR site, at EL, $C_{max} = C_{16}$, WM, $C_{max} = C_{17}$ and at RU, $C_{max} = C_{17}$,
392 respectively.

393

394

395 **3.2.2 The ratios of n-alkanes/n-alkanals**

396 Diesel engine emission studies have been conducted previously in our group; details of the engine set
397 up and exhaust sampling system are given elsewhere (Alam et al., 2016b). Briefly, the steady-state
398 diesel engine operating conditions were at a load of 5.90 bar mean effective pressure (BMEP) and a
399 speed of 1800 revolutions per minute (RPM), and samples (n=14) were collected both before a diesel
400 oxidation catalyst (DOC) and after a diesel particulate filter (DPF). The n-alkanes (C₁₂ - C₃₇) and 1-
401 alkanals (C₉ - C₁₈) were quantified in the particle samples, while n-alkanones were not identified
402 because their concentrations were lower than the limits of (detection 0.01–0.15 ng m⁻³). The emission
403 concentrations of n-alkanals ranged from 7.10 to 53.2 µg m⁻³ (before DOC) and 1.20 to 11.5 µg m⁻³
404 (after DPF), respectively, and the ratios of alkanes/alkanals (C₁₃-C₁₈) with the same carbon atom
405 numbers ranged from 0.15 to 0.23 (before DOC) and 0.52 to 7.60 (after DPF). The n-alkane/n-alkanal
406 (C₁₃-C₁₈) ratio at MR ranged from 0.30 to 5.7, while average ratios of 14.9 (RU), 11.5 (WM) and
407 14.7 (EL) were obtained, respectively. The similarity of the n-alkanes/n-alkanal ratio between MR
408 and the engine studies (after DPF) strongly suggests that diesel vehicle emissions were the main
409 source of alkanals at MR. The higher ratios at the other sites may be due to greater airmass aging and
410 loss of alkanals due to their higher reactivity (Chacon-Madrid and Donahue, 2011; Chacon-Madrid
411 et al., 2010).

412

413 The emission factors of total alkanes from diesel engines are reported to be 7 times greater than
414 gasoline engines (Perrone et al., 2014), with n-alkanals with carbon atoms numbering lower than C₁₁
415 being quantified in the exhaust from gasoline engines (Schauer et al., 2002b; Gentner et al., 2013).
416 The n-alkane/n-alkanal (C₈-C₁₀) ratio with the same carbon numbers ranged from 5.60 to 14.3

417 (Schauer et al., 2002b), suggesting that gasoline combustion may be another potential source of
418 atmospheric n-alkanals.

419

420 **3.2.3 Correlation analysis**

421 Insights into the sources of carbonyls can be gained from intra-site correlation analysis with black
422 carbon (BC) and NO_x. This is more informative than comparisons between sites when sampling did
423 not take place simultaneously, as concentrations are strongly affected by weather conditions, making
424 inter-site comparisons difficult to interpret. In London, both black carbon and NO_x arise very
425 substantially from diesel vehicle emissions (Liu et al., 2014; Harrison et al., 2012; Harrison and
426 Beddows, 2017), and hence these are good measures of road traffic activity. The concentrations of
427 BC were simultaneously determined by the online instruments during the sampling periods, with the
428 average concentrations of 1.34, 1.94 and 3.58 µg m⁻³ at the RU, WM and MR sites, respectively.

429 The data for NO_x were provided by the national network sites, with the average concentrations of
430 23.4 and 202 µg m⁻³ at the EL and MR sites, respectively. At the MR site, the concentrations of BC
431 and NO_x averaged 5.00 µg m⁻³ and 281 µg m⁻³ when southerly winds were dominant compared to
432 2.60 and 128 µg m⁻³ for northerly winds. All correlations were carried out with the sum of particle
433 and vapour phases for the carbonyl compounds, and strong ($r^2 = 0.87$) and weak ($r^2 = 0.12$)
434 correlations between BC and NO_x were obtained when the southerly and northerly winds were
435 prevalent at MR, respectively. Marylebone Road is a street canyon site where a vortex circulation is
436 established by the wind. The effect is that on northerly wind sectors the sampling site on the southern
437 side of the road samples near-background air, while on southerly wind sectors, the traffic pollution
438 is carried to the sampling site, leading to elevated pollution levels affected heavily by the traffic

439 emissions. The strong correlation between BC and NO_x with southerly wind sectors is a reflection
440 of their emission from road traffic. In addition, the correlations between n-alkanals (C₈-C₂₀) and BC,
441 and between n-alkanals (C₈-C₂₀) and NO_x were calculated to assess the contribution of vehicular
442 emissions (Table S43). The results showed that the correlations (r^2) between n-alkanals and BC
443 gradually decreased from 0.61 (C₉) to 0.34 (C₂₀) at MR when the southerly winds were prevalent,
444 indicating that the distribution of n-alkanals, and especially the lower MW compounds, was
445 significantly impacted by the vehicular exhaust emissions. The average correlations at MR
446 (southerly winds) between n-alkanals and BC, and between n-alkanals and NO_x were $r^2 = 0.47$ and
447 $r^2 = 0.32$, respectively. These moderate correlations demonstrated that the vehicular emissions were
448 a source of n-alkanals at MR, and contribute to the high background concentrations of n-alkanals in
449 London. The other probable sources of n-alkanals include cooking emissions, wood burning,
450 photooxidation of hydrocarbons and industrial emissions. Poorer correlations between n-alkanals
451 and BC (average $r^2 = 0.15$), and between n-alkanals and NO_x (average $r^2 = 0.15$) were observed at
452 MR in the north London background air sampled when northerly winds were prevalent. There were
453 very weak correlations (average $r^2 < 0.10$) between n-alkanals and BC, and between n-alkanals and
454 NO_x at the RU, WM and EL sites, which may be attributable to the high chemical reactivity of n-
455 alkanals. High concentrations of furanones (γ -lactones) are generated via the photo-oxidation
456 reaction of n-alkanals (Alves et al., 2001), and the total concentrations (particle and gas) were up to
457 376, 279, 347 and 318 ng m⁻³ at RU, WM, WL, and MR, respectively for the sum of furanone
458 homologues (from 5-propyldihydro-2(3H)-furanone to 5-tetradecyldihydro-2(3H)-furanone).

459

460 The relationships (r^2 values) between BC and NO_x and the n-alkan-2-ones were low at all sites, but
461 notably higher with southerly winds at MR (average $r^2 = 0.33$ and 0.35 for BC and NO_x respectively)
462 than for northerly winds ($r^2 = 0.16$ and 0.03 respectively). This is strongly suggestive of a
463 contribution from vehicle exhaust to n-alkan-2-one concentrations, but smaller than that for n-
464 alkanals. In the case of the n-alkan-3-ones, correlations averaged $r^2 = 0.25$ with BC and $r^2 = 0.21$ for
465 NO_x in southerly winds, compared to $r^2 = 0.08$ and $r^2 = 0.05$ respectively for northerly winds. This
466 is also suggestive of a small, but not negligible contribution of vehicle emissions to n-alkan-3-ones.
467 The very low correlations observed in background air for both n-alkan-2-ones and n-alkan-3-ones
468 with BC and NO_x are suggestive of the importance of non-traffic sources, probably including
469 oxidation of n-alkanes. Both compound groups were below detection limit in the analyses of diesel
470 exhaust. The considerable predominance of n-alkan-2-one over n-alkan-3-one concentrations may
471 be indicative of a formation pathway from oxidation of condensed phase n-alkanes, but this is
472 speculative as primary emissions may be dominant.

473

474 3.3 Gas and Particle Phase Partitioning

475 The partitioning coefficient K_p between particles and vapour ($\geq C_{10}$) was calculated in this study
476 according to the following equation defined by Pankow (1994):
477

$$478 K_p = \frac{C_p}{C_g * TSP}$$

479

480 Where, C_p and C_g ($\mu\text{g m}^{-3}$) are the concentration of the compounds in the particulate phase and
481 gaseous phase, respectively. TSP is the concentration of total suspended particulate matter ($\mu\text{g m}^{-3}$),

482 which was estimated from the PM₁₀ concentration (PM₁₀/TSP = 0.80), and daily average PM₁₀
483 concentrations were taken from the national network sites (see Table S5). The partitioning
484 coefficients K_p calculated from our data and the percentages in the particulate form are presented in
485 Table 2. For the three types of carbonyls, the n-alkanals >C₁₆, n-alkan-2-ones >C₁₉, and n-alkan-3-
486 ones > C₁₈ the vapour concentrations were below detection limit, and the partitioning into the
487 particulate phase gradually increased from C₈ to high molecular weight compounds.

488

489 Log K_p was regressed against vapour pressure (VP_T) for the relevant temperature derived from
490 UManSysProp (<http://umansysprop.seaes.manchester.ac.uk/>) according to the following equation:

491

492 $\text{Log } K_p = m \log(VP_T) + b$

493

494 The calculated log K_p versus log (VP_T) for the three types of carbonyls was calculated for each day,
495 and the results appear in the Table S₆₄. Data from four sites were over the temperature range 0.40–
496 15.3 °C. A good fit to the data for n-alkan-2-ones ($r^2 = 0.5455$ –0.94 at RU, 0.64–0.93 at WM, 0.4345–
497 0.9594 at EL and 0.45–0.890.36–0.88 at MR) was obtained. It is notable that the fit to the regression
498 equation as indicated by the r^2 value is appreciably higher at the MR site than at the other sites,
499 especially in the case of the alkan-3-ones ([Table S6](#)). This is not easily explained, except perhaps by
500 an increased particle surface area at the MR site which may enhance the kinetics of gas-particle
501 exchange, leading to partitioning which is closer to equilibrium.

502

503 According to theory, the gradient of the plot of $\log K_P$ versus $\log (VP_T)$ should be -1 (Pankow,
504 1994). However, many measurement datasets for a number of semi-volatile compound groups
505 including n-alkanes (Cincinelli et al., 2007; Karanasiou et al., 2007; Mandalakis et al., 2002) and
506 PAH (Callen et al., 2008; Wang et al., 2011; Ma et al., 2011; Mandalakis et al., 2002) show a range
507 of values, often around -0.5, but ranging to below -1, and in some cases positive. Callen et al.,
508 (2008) discuss the reasons for deviation from a value of -1, which include a lack of equilibrium,
509 absorption into the organic matter (shallow than -0.6), adsorption processes (steeper than -1), and
510 the averaging of conditions across a range of temperatures during a sampling period.

511

512 Our data for alkan-2-ones show high r^2 values and values of gradient (m) in the range of the
513 literature for other groups of semi-volatile compounds. Average gradients at the four sites ranged
514 from -0.46 to -0.26. The alkan-3-ones show generally considerably lower values of r^2 and average
515 values of gradient at the four sites of -0.43 to -0.23. This poorer correlation could be the result of
516 lower analytical precision. The n-alkanals show still lower values of r^2 , and more variable and
517 shallower values of slope. Mean slopes for the four sites ranged from -0.23 to -0.16. There were
518 no positive daily values. The lower r^2 may be a result of disequilibrium for the alkanals which are
519 dominated by primary emissions, and are also more reactive. It might also reflect a role for aqueous
520 aerosol as an absorbing medium for these compounds containing a significant polar moiety, which
521 would lead to deviations from the Pankow (1994) theory, and more variable behaviour as the
522 availability of aqueous particles into which to partition would depend upon relative humidity, which
523 is itself highly variable.

524

525 Samples were collected over 24-hour periods and hence the diurnal variation of temperature may be
526 relevant. Temperature data were taken from Heathrow Airport to the west of London and did not
527 show large diurnal fluctuations, so this should not be a major factor. The average diurnal
528 temperature range based upon hourly data was 6.9°C.

529

530 The lower molecular weight n-alkanals show a much higher percentage in the condensed phase than
531 the ketone groups (Table 2).

532

533 This greater propensity to partition into the particles is unexpected, as the vapour pressures of the
534 alkanals are very similar to those of the ketones. It might possibly reflect a greater affinity of the
535 alkanals for solvation by water molecules, leading to increased partition into aqueous aerosol.

536

537 **4. CONCLUSIONS**

538 Three groups of carbonyl compounds were determined in the particle and gaseous phase in London
539 and concentrations are reported for n-alkanals (C₈-C₂₀), n-alkan-2-ones (C₈-C₂₆) and n-alkan-3-ones
540 (C₈-C₁₉). The Marylebone Road site has the highest concentration of particle-bound n-alkanals, and
541 the average total concentration was up to 682 ng m⁻³, followed by 167 ng m⁻³ at EL, 117 ng m⁻³ at
542 WM and 82.6 ng m⁻³ at RU. The particulate n-alkanals were abundant in all samples at all four
543 measurement sites, accounting for more than 56.3% of total particle carbonyls. In addition, the
544 average total particle concentrations of n-alkan-2-ones and n-alkan-3-ones at four measurement sites
545 were in the range of 58.5-186 ng m⁻³ and 5.65-39.4 ng m⁻³, respectively. Diagnostic criteria,

546 including molecular distribution, CPI, C_{max} , ratios and correlations, were used to assess the sources
547 and their contributions to carbonyl compounds. The three groups of carbonyls have similar
548 molecular distributions and C_{max} values at the four measurement sites, and their low CPI values
549 (0.41-1.57) at the four sites indicate a weak biogenic input during sampling campaigns. Heavily
550 traffic-influenced air and urban background air were measured at the MR site when southerly and
551 northerly winds were prevalent respectively; correlations of $r^2 = 0.47$ and $r^2=0.32$ were obtained
552 between n-alkanals and BC, and between between n-alkanals and NO_x , respectively in southerly
553 winds. Vehicle emissions appear to be an important source of n-alkanals, which is confirmed by the
554 similar ratios of n-alkanes/n-alkanals measured at MR (0.30-5.75) and in diesel engine exhaust
555 studies (0.52-7.6), resulting in a high background concentration in London. In addition, the OH-
556 initiated heterogeneous reactions of n-alkanes appear to be important sources of n-alkanones, even
557 though weak contributions from vehicular exhaust emissions were suggested by correlation analysis
558 with BC and NO_x in southerly winds at MR. Anthropogenic primary sources such as cooking
559 (Abdullahi et al., 2013) may account for a proportion of the alkan-2-one and alkan-3-one
560 concentrations measured in London, in addition to the secondary contribution from alkane oxidation.
561 Any contribution from cooking or wood combustion is likely to be small, or the CPI would be greater.
562

563 In addition, the partitioning coefficients of carbonyls were determined from the relative proportions
564 of the particle and gaseous phases of individual compounds.~~The results of field measurements of~~
565 ~~partitioning between particle and vapour phases showed and~~ generally showed a better fit at MR
566 than at the other three sites. ~~The n-alkan-2-ones have a better fit at four sites than the n-alkanals and~~
567 ~~n-alkan-3-ones, with $r^2 = 0.72$ (0.49-0.57) at RU, 0.76 (0.55-0.87) at WM, 0.74 (0.43-0.95) EL and~~

568 0.70 (0.45–0.89) at MR, respectively in a regression of $\log K_p$ versus the compound vapour
569 pressure. Fits to the Pankow (1994) model were best for alkan-2-ones and. This is most likely
570 reflects the slow formation of the alkan-2-ones as secondary constituents, closer to phase equilibrium
571 than the largely emitted predominantly emitted and more reactive alkanals which would be spatially
572 far more variable. The higher r^2 values for the alkan-2-ones than alkan-3-ones may reflect the
573 higher concentrations, and hence better analytical precision for the former compound group.

574

575 **ACKNOWLEDGEMENTS**

576 Primary collection of samples took place during the FASTER project which was funded by the
577 European Research Council (ERC-2012-AdG, Proposal No. 320821). The authors would also like
578 to thank the China Scholarship Council (CSC) for support to R.L., and the Natural Environment
579 Research Council for support under the Air Pollution and Human Health (APHH) programme
580 (NE/N007190/1).

581 **REFERENCE**

582

583 Abdullahi, K.L., Delgado-Saborit, J.M., and R.M. Harrison: Emissions and indoor concentrations
584 of particulate matter and its specific chemical components from cooking: A review, *Atmos.*
585 *Environ.*, 71, 260-294, <http://dx.doi.org/10.1016/j.atmosenv.2013.01.061>, 2013.

586

587 Alam, M. S., Stark, C., and Harrison, R. M.: Using variable ionization energy time-of-flight mass
588 spectrometry with comprehensive GC \times GC to identify isomeric species, *Anal. Chem.*, 88, 4211-
589 4220, <http://www.doi.org/10.1021/acs.analchem.5b03122>, 2016a.

590

591 Alam, M. S., Zeraati-Rezaei, S., Stark, C. P., Liang, Z., Xu, H., and Harrison, R. M.: The
592 characterisation of diesel exhaust particles - composition, size distribution and partitioning,
593 *Faraday. Discuss.*, 189, 69-84, <http://www.doi.org/10.1039/C5FD00185D>, 2016b.

594

595 Alam, M. S., Zeraati-Rezaei, S., Liang, Z., Stark, C., Xu, H., MacKenzie, A. R., and Harrison, R.
596 M.: Mapping and quantifying isomer sets of hydrocarbons (\geq C 12) in diesel exhaust, lubricating oil
597 and diesel fuel samples using GC \times GC-ToF-MS, *Atmos. Meas. Tech.*, 11, 3047,
598 <https://doi.org/10.5194/amt-11-3047-2018>, 2018.

599

600 Algrim, L. B., and Ziemann, P. J.: Effect of the Keto Group on yields and composition of organic
601 aerosol formed from OH radical-initiated reactions of ketones in the presence of NO_x, *J. Phys.*
602 *Chem. A.*, 120, 6978-6989, <http://www.doi.org/10.1021/acs.jpca.6b05839>, 2016.

603

604 Alves, C., Pio, C., and Duarte, A.: Composition of extractable organic matter of air particles from
605 rural and urban Portuguese areas, *Atmos. Environ.*, 35, 5485-5496, [https://doi.org/10.1016/S1352-2310\(01\)00243-6](https://doi.org/10.1016/S1352-2310(01)00243-6), 2001.

607

608 Andreou, G., and Rapsomanikis, S.: Origins of n-alkanes, carbonyl compounds and molecular
609 biomarkers in atmospheric fine and coarse particles of Athens, Greece, *Sci. Total. Environ.*, 407,
610 5750-5760, <http://dx.doi.org/10.1016/j.scitotenv.2009.07.019>, 2009.

611

612 Aschmann, S. M., Arey, J., and Atkinson, R.: Atmospheric chemistry of three C10 alkanes, *J. Phys.*
613 *Chem. A.*, 105, 7598-7606, <http://www.doi.org/10.1021/jp010909j>, 2001.

614

615 Bray, E., and Evans, E.: Distribution of n-paraffins as a clue to recognition of source beds,
616 *Geochim. Cosmochim. Ac.*, 22, 2-15, [https://doi.org/10.1016/0016-7037\(61\)90069-2](https://doi.org/10.1016/0016-7037(61)90069-2), 1961.

617

618 Callen, M. S., de la Cruz, M. T., opez, J. M., Murillo, R., Navarro, M. V., and Mastral, A. M.:
619 Some inferences on the mechanism of atmospheric gas/particle partitioning of polycyclic aromatic
620 hydrocarbons (PAH) at Zaragoza (Spain), *Chemosphere*, 73, 1357-1365, 2008.

621

622 Chacon-Madrid, H., and Donahue, N.: Fragmentation vs. functionalization: chemical aging and
623 organic aerosol formation, *Atmos. Chem. Phys.*, 11, 10553-10563, <https://doi.org/10.5194/acp-11-10553-2011>, 2011.

625 Chacon-Madrid, H. J., Presto, A. A., and Donahue, N. M.: Functionalization vs. fragmentation: n-
626 aldehyde oxidation mechanisms and secondary organic aerosol formation, *Phys. Chem. Chem.
627 Phys.*, 12, 13975-13982, <http://www.doi.org/10.1039/C0CP00200C>, 2010.

628 Cheng, Y., Li, S.-M., Leithead, A., and Brook, J. R.: Spatial and diurnal distributions of n-alkanes
629 and n-alkan-2-ones on PM 2.5 aerosols in the Lower Fraser Valley, Canada, *Atmos. Environ.*, 40,
630 2706-2720, <https://doi.org/10.1016/j.atmosenv.2005.11.066>, 2006.

631

632 Cincinelli, A., Del Bubba, M., Martellini, T., Gambaro, A., and Lepri, L.: Gas-particle
633 concentration and distribution of *n*-alkanes and polycyclic aromatic hydrocarbons in the atmosphere
634 of Prato (Italy), *Chemosphere*, 68, 472-478, 2007.

635

636 Duan, H., Liu, X., Yan, M., Wu, Y., and Liu, Z.: Characteristics of carbonyls and volatile organic
637 compounds (VOCs) in residences in Beijing, China, *Front. Env. Sci. Eng.*, 10, 73-84,
638 <http://www.doi.org/10.1007/s11783-014-0743-0>, 2016.

639

640 Gentner, D. R., Worton, D. R., Isaacman, G., Davis, L. C., Dallmann, T. R., Wood, E. C., Herndon,
641 S. C., Goldstein, A. H., and Harley, R. A.: Chemical composition of gas-phase organic carbon
642 emissions from motor vehicles and implications for ozone production, *Environ. Sci. technol.*, 47,
643 11837-11848, <http://www.doi.org/10.1021/es401470e>, 2013.

644

645 Gogou, A., Stratigakis, N., Kanakidou, M., and Stephanou, E. G.: Organic aerosols in Eastern
646 Mediterranean: components source reconciliation by using molecular markers and atmospheric back
647 trajectories, *Org. Geochem.*, 25, 79-96, [https://doi.org/10.1016/S0146-6380\(96\)00105-2](https://doi.org/10.1016/S0146-6380(96)00105-2), 1996.

648

649 Han, Y., Kawamura, K., Chen, Q., and Mochida, M.: Formation of high-molecular-weight
650 compounds via the heterogeneous reactions of gaseous C8–C10 n-aldehydes in the presence of
651 atmospheric aerosol components, *Atmos. Environ.*, 126, 290-297,
652 <http://dx.doi.org/10.1016/j.atmosenv.2015.11.050>, 2016.

653

654 Harrison, R., Dall'Osto, M., Beddows, D., Thorpe, A., Bloss, W., Allan, J., Coe, H., Dorsey, J.,
655 Gallagher, M., and Martin, C.: Atmospheric chemistry and physics in the atmosphere of a
656 developed megacity (London): an overview of the REPARTEE experiment and its conclusions,
657 *Atmos. Chem. Phys.*, 12, 3065-3114, <https://doi.org/10.5194/acp-12-3065-2012>, 2012.

658

659 Harrison, R. M., and Beddows, D. C.: Efficacy of recent emissions controls on road vehicles in
660 Europe and implications for public health, *Sci. Rep-UK.*, 7, 1152,
661 <http://www.doi.org/10.1038/s41598-017-01135-2>, 2017.

662

663 Karanasiou, A. A., Sitaras, I. E., Siskos, P. A., and Eleftheriadis, K.: Size distribution and sources
664 of trace metals and *n*-alkanes in the Athens urban aerosol during summer, *Atmos. Environ.*, 41,
665 2368-2381, 2007.

666

667 Kwok, E. S., and Atkinson, R.: Estimation of hydroxyl radical reaction rate constants for gas-phase
668 organic compounds using a structure-reactivity relationship: an update, *Atmos. Environ.*, 29, 1685-
669 1695, [https://doi.org/10.1016/1352-2310\(95\)00069-B](https://doi.org/10.1016/1352-2310(95)00069-B), 1995.

670
671 Lim, Y. B., and Ziemann, P.J.: Chemistry of secondary organic aerosol formation from OH
672 radical-initiated reactions of linear, branched, and cyclic alkanes in the presence of NO_x, *Aerosol*
673 *Sci. Technol.*, 43, 604-619, <https://doi.org/10.1080/02786820902802567>, 2009.

674
675 Liu, D., Allan, J., Young, D., Coe, H., Beddows, D., Fleming, Z., Flynn, M., Gallagher, M.,
676 Harrison, R., and Lee, J.: Size distribution, mixing state and source apportionments of black carbon
677 aerosols in London during winter time, *Atmos. Chem. Phys.*, 14, <https://doi.org/10.5194/acp-14-10061-2014>, 2014.

679
680 Ma, W.-L., Sun, D.-Z., Shen, W.-G., Yang, M., Qi, H., Liu, L.-Y., Shen, J.-M., and Li, Y.-F.:
681 Atmospheric concentrations, sources and gas-particle partitioning of PAHs in Beijing after the 29th
682 Olympic Games, *Environ. Pollut.*, 159, 1794-1801, 2011.

683
684 Mandalakis, M., Tsapakis, M., Tsoga, A., and Stephanou, E. G.: Gas-particle concentrations and
685 distribution of aliphatic hydrocarbons, PAHs, PCBs and PCDD/Fs in the atmosphere of Athens
686 (Greece), *Atmos. Environ.*, 36, 4023-4034, 2002.

687
688 Oliveira, T. S., Pio, C., Alves, C. A., Silvestre, A. J., Evtyugina, M., Afonso, J., Fialho, P., Legrand,
689 M., Puxbaum, H., and Gelencsér, A.: Seasonal variation of particulate lipophilic organic
690 compounds at nonurban sites in Europe, *J. Geophys. Res-Atmos.*, 112,
691 <https://doi.org/10.1029/2007JD008504> 2007.

692
693 Oros, D. R., and Simoneit, B. R. T.: Identification and emission rates of molecular tracers in coal
694 smoke particulate matter, *Fuel.*, 79, 515-536, [http://dx.doi.org/10.1016/S0016-2361\(99\)00153-2](http://dx.doi.org/10.1016/S0016-2361(99)00153-2),
695 2000.

696
697 Pankow, J. F.: An absorption model of gas/particle partitioning of organic compounds in the
698 atmosphere, *Atmos. Environ.*, 28, 185-188, [https://doi.org/10.1016/1352-2310\(94\)90093-0](https://doi.org/10.1016/1352-2310(94)90093-0), 1994.

699
700 Perrone, M. G., Carbone, C., Faedo, D., Ferrero, L., Maggioni, A., Sangiorgi, G., and Bolzacchini,
701 E.: Exhaust emissions of polycyclic aromatic hydrocarbons, n-alkanes and phenols from vehicles
702 coming within different European classes, *Atmos. Environ.*, 82, 391-400,
703 <https://doi.org/10.1016/j.atmosenv.2013.10.040>, 2014.

704
705 Rogge, W. F., Hildemann, L. M., Mazurek, M. A., and Cass, G. R.: Sources of fine organic aerosol.
706 9. Pine, oak, and synthetic log combustion in residential fireplaces, *Environ. Sci. Technol.*, 32, 13-
707 22, <http://www.doi.org/10.1021/es960930b>, 1998.

708
709
710 Ruehl, C. R., Nah, T., Isaacman, G., Worton, D. R., Chan, A. W. H., Kolesar, K. R., Cappa, C. D.,
711 Goldstein, A. H., and Wilson, K. R.: The influence of molecular structure and aerosol phase on the
712 heterogeneous oxidation of normal and branched alkanes by OH, *J. Phys. Chem. A.*, 117, 3990-
713 4000, <http://www.doi.org/10.1021/jp401888q>, 2013.

714

715 Schauer, J. J., Kleeman M. J., Cass, G. R., and Simoneit, B. R. T.: Measurement of emissions
716 from air pollution sources. 2. C1 through C30 organic compounds from medium duty diesel trucks,
717 Environ. Sci. Technol., 33, 1578-1587, 10.1021/es980081n, 1999a.

718

719 Schauer, J. J., Kleeman, M. J., Cass, G. R., and Simoneit, B. R. T.: Measurement of emissions from
720 air pollution sources. 1. C1 through C29 organic compounds from meat charbroiling, Environ. Sci.
721 Technol., 33, 1566-1577, <http://www.doi.org/10.1021/es980076j>, 1999b.

722

723 Schauer, J. J., Kleeman, M. J., Cass, G. R., and Simoneit, B. R. T.: Measurement of emissions from
724 air pollution sources. 3. C1-C29 organic compounds from fireplace combustion of wood, Environ.
725 Sci. technol., 35, 1716-1728, <http://www.doi.org/10.1021/es001331e>, 2001.

726

727 Schauer, J. J., Kleeman, M. J., Cass, G. R., and Simoneit, B. R. T.: Measurement of emissions from
728 air pollution sources. 4. C1-C27 organic compounds from cooking with seed oils, Environ. Sci.
729 Technol., 36, 567-575, <http://www.doi.org/10.1021/es002053m>, 2002a.

730

731 Schauer, J. J., Kleeman, M. J., Cass, G. R., and Simoneit, B. R. T.: Measurement of emissions from
732 air pollution sources. 5. C1-C32 organic compounds from gasoline-powered motor vehicles,
733 Environ. Sci. Technol., 36, 1169-1180, <http://www.doi.org/10.1021/es0108077>, 2002b.

734

735 Schilling Fahnestock, K. A., Yee, L. D., Loza, C. L., Coggon, M. M., Schwantes, R., Zhang, X.,
736 Dalleska, N. F., and Seinfeld, J. H.: Secondary organic aerosol composition from C12 alkanes, J.
737 Phys. Chem. A., 119, 4281-4297, <http://www.doi.org/10.1021/jp501779w>, 2015.

738

739 Simoneit, B. R. T., Cox, R. E., and Standley, L. J.: Organic matter of the troposphere - IV. Lipids in
740 harmattan aerosols of Nigeria, Atmos. Environ., 22, 983-1004, [https://doi.org/10.1016/0004-6981\(88\)90276-4](https://doi.org/10.1016/0004-6981(88)90276-4), 1967.

741

742

743 UK-Air, <https://uk-air.defra.gov.uk>, last accessed 16 December 2018.

744

745 Wang, W., Massey Simonich, S. L., Wang, W., Giri, B., Zhao, J., Xue, M., Cao, J., Lu, X. and Tao, S.: Atmospheric polycyclic aromatic hydrocarbon concentrations and gas/particle partitioning at background, rural village and urban sites in the North China Plain, Atmos. Res., 99, 197-206, 2011.

746

747

748

749 Yee, L. D., Craven, J. S., Loza, C. L., Schilling, K. A., Ng, N. L., Canagaratna, M. R., Ziemann, P.
750 J., Flagan, R. C., and Seinfeld, J. H.: Secondary organic aerosol formation from low-NO_x
751 photooxidation of dodecane: Evolution of multigeneration gas-phase chemistry and aerosol
752 composition, J. Phys. Chem. A., 116, 6211-6230, <http://www.doi.org/10.1021/jp211531h>, 2012.

753

754 Zhang, H., Worton, D. R., Shen, S., Nah, T., Isaacman-VanWertz, G., Wilson, K. R., and Goldstein,
755 A. H.: Fundamental time scales governing organic aerosol multiphase partitioning and oxidative
756 aging, Environ. Sci. technol., 49, 9768-9777, <http://www.doi.org/10.1021/acs.est.5b02115>, 2015.

757

758 Zhao, Y., Hu, M., Slanina, S., and Zhang, Y.: The molecular distribution of fine particulate organic
759 matter emitted from Western-style fast food cooking, *Atmos. Environ.*, 41, 8163-8171,
760 <http://dx.doi.org/10.1016/j.atmosenv.2007.06.029>, 2007a.

761

762 Zhao, Y., Hu, M., Slanina, S., and Zhang, Y.: Chemical compositions of fine particulate organic
763 matter emitted from Chinese cooking, *Environ. Sci. Technol.*, 41, 99-105,
764 <http://www.doi.org/10.1021/es0614518>, 2007b.

765

766 Ziemann, P. J.: Effects of molecular structure on the chemistry of aerosols formation from the
767 OH-radical-initiated oxidation of alkanes and alkenes, *Intl. Rev. Phys. Chem.*, 30, 161-195,
768 <https://doi.org/10.1080/0144235X.2010.550728>, 2011.

769

770

771

772 **TABLE LEGENDS**

773

774 Table 1. The carbon preference index (CPI) and C_{max} for n-alkanals, n-alkan-2-ones, and
775 n-alkan-3-ones in this study and published data.

776

777 Table 2. Percentages of particle phase form and the partitioning coefficient K_p .

778

779 **FIGURE LEGENDS**

780

781 Figure 1. Map of the sampling sites. RU-Regents University (15 m above ground); WM-
782 University of Westminster (20 m above ground); EL-Eltham; MR-Marylebone Road
783 (south side).

784

785 Figure 32. Time series of particle-bound \sum n-alkanals, \sum n-alkan-2-ones and \sum n-alkan-3-ones at
786 RU, WM, EL, and MR sites.

787

788 Figure 23. The average total concentration of particle-bound n-alkanals (C_8-C_{20}), n-alkan-2-ones
789 (C_8-C_{26}), and n-alkan-3-ones (C_8-C_{19}), for each sampling period and site. The error bars
790 indicate one standard deviation.

791

792 Figure 3. Time series of particle bound \sum n alkanals, \sum n alkan 2 ones and \sum n alkan 3 ones at
793 RU, WM, EL, and MR sites.

794

795 Figure 4. The molecular distribution of particle-bound carbonyl compounds at four sites (RU,
796 WM, EL, and MR).

797

798

799

Table 1. The carbon preference index (CPI) and C_{\max} for n-alkanals, n-alkan-2-ones, and n-alkan-3-ones in this study and published data.

Location	Sampling period	n-alkanals		n-alkan-2-ones		n-alkan-3-ones		Reference
		CPI	C_{\max}	CPI	C_{\max}	CPI	C_{\max}	
RU, surrounded by Regent's Park, 15 m above ground	23 Jan - 19 Feb	0.52	C_8	1.23	C_{19}	1.30	C_{17}	Present study
WM, 20 m above ground	24 Jan - 20 Feb	0.41	C_8	0.99	C_{20}	1.26	C_{17}	Present study
EL, suburb of London	23 Feb - 21 Mar	0.71	C_8	1.57	C_{20}	1.04	C_{16}	Present study
MR, adjacent to Marylebone road	22 Mar - 18 Apr	1.07	C_8	0.57	C_{16}	1.12	C_{16}	Present study
Athens, Athinas St. Urban roadside	August March	1.49	C_{15}, C_{17}	1.09 3.26	C_{18}, C_{21}, C_{19} C_{21}, C_{19}, C_{20}			(Andreou and Rapsomanikis, 2009)
Athens, AEDA, Urban, 20 m above ground	March			2.41	C_{19}, C_{18}, C_{20}			(Andreou and Rapsomanikis, 2009)
Heraklion, Greece Urban 15 m above ground	Spring /summer	0.80–1.40	C_{26}, C_{28}	1.30–1.80	C_{23}, C_{29}, C_{31}			(Gogou et al., 1996)
Vancouver, Canada Roadway tunnel				1.33	C_{17}, C_{19}			(Cheng et al., 2006)
Aveiro, Portugal Suburban	Summer Winter		C_{22}, C_{23}, C_{26}		C_{26}, C_{28}, C_{30}			(Oliveira et al., 2007)
K-Puszta, Hungary	Summer		C_{24}, C_{26}, C_{28}		C_{24}, C_{26}, C_{28}			

Table 2. Percentages of particle phase form and the partitioning coefficient Kp ($\text{m}^3 \mu\text{g}^{-1}$).

	RU						WM					
	n-alkanals		n-alkan-2-ones		n-alkan-3-ones		n-alkanals		n-alkan-2-ones		n-alkan-3-ones	
	%	Kp	%	Kp	%	Kp	%	Kp	%	Kp	%	Kp
C ₈	82.9	1.16E-04	18.4	5.37E-06	23.9	7.47E-06	80.2	9.09E-05	13.3	3.43E-06	34.1	1.16E-05
C ₉	69.2	5.37E-05	14.5	4.03E-06	16.6	4.74E-06	60.5	3.43E-05	15.6	4.16E-06	28.7	9.05E-06
C ₁₀	75.3	7.27E-05	13.6	3.77E-06	7.43	1.92E-06	82.1	1.03E-04	14.4	3.77E-06	23.3	6.82E-06
C ₁₁	45.5	1.99E-05	21.4	6.49E-06	12.8	3.49E-06	62.4	3.72E-05	20.1	5.65E-06	36.3	1.28E-05
C ₁₂	74.8	7.08E-05	25.0	7.96E-06	31.3	1.09E-05	73.7	6.29E-05	28.8	9.07E-06	22.7	6.60E-06
C ₁₃	82.9	1.15E-04	61.0	3.74E-05	35.4	1.31E-05	82.2	1.04E-04	48.9	2.14E-05	62.5	3.74E-05
C ₁₄	82.8	1.15E-04	49.5	2.34E-05	35.5	1.31E-05	75.8	7.04E-05	31.8	1.05E-05	25.6	7.74E-06
C ₁₅	99.5	5.01E-03	84.1	1.26E-04	50.5	2.44E-05	*		85.0	1.27E-04	68.5	4.87E-05
C ₁₆	*		91.4	2.53E-04	70.3	5.64E-05	*		89.6	1.93E-04	91.7	2.47E-04
C ₁₇	*		91.5	2.55E-04	*		*		85.9	1.36E-04	91.5	2.42E-04
C ₁₈	*		94.1	3.80E-04	*		*		84.8	1.26E-04	99.4	4.02E-03
C ₁₉	*		99.1	2.69E-03			*		*			
C ₂₀	*	*					*		*		*	
C ₂₁		*							*			
C ₂₂		*							*			
C ₂₃		*							*			
C ₂₄		*							*			
C ₂₅		*							*			
C ₂₆		*							*			

	EI						MR					
	n-alkanals		n-alkan-2-ones		n-alkan-3-ones		n-alkanals		n-alkan-2-ones		n-alkan-3-ones	
	%	K _p	%	K _p	%	K _p	%	K _p	%	K _p	%	K _p
C ₈	92.7	6.53E-04	24.9	1.72E-05	31.9	2.43E-05	90.0	2.94E-04	28.2	1.28E-05	43.0	2.46E-05
C ₉	92.2	6.16E-04	38.0	3.18E-05	44.4	4.15E-05	89.9	2.89E-04	27.0	1.20E-05	39.1	2.09E-05
C ₁₀	90.5	4.96E-04	47.6	4.70E-05	47.0	4.59E-05	91.7	3.62E-04	61.1	5.12E-05	20.4	8.33E-06
C ₁₁	87.0	3.47E-04	72.3	1.35E-04	81.9	2.34E-04	87.4	2.26E-04	50.2	3.28E-05	33.1	1.61E-05
C ₁₂	92.9	6.73E-04	83.4	2.60E-04	66.4	1.02E-04	93.0	4.30E-04	88.5	2.51E-04	28.1	1.28E-05
C ₁₃	95.6	1.12E-03	82.2	2.40E-04	65.7	9.92E-05	96.1	8.04E-04	87.7	2.33E-04	46.2	2.79E-05
C ₁₄	91.4	5.52E-04	90.3	4.80E-04	59.1	7.48E-05	95.2	6.51E-04	95.9	7.61E-04	72.0	8.38E-05
C ₁₅	96.7	1.53E-03	94.5	8.98E-04	84.4	2.80E-04	*		96.9	1.02E-03	83.8	1.69E-04
C ₁₆	*		96.7	1.41E-03	89.0	4.18E-04	*		96.4	8.70E-04	88.0	2.38E-04
C ₁₇	*		95.1	1.00E-03	81.5	2.28E-04	*		96.0	7.73E-04	88.0	2.39E-04
C ₁₈	*		64.6	9.44E-05	85.0	2.93E-04	*		92.5	4.04E-04	*	
C ₁₉	*		*				*		*		*	
C ₂₀	*		*				*		*		*	
C ₂₁			*						*		*	
C ₂₂			*						*		*	
C ₂₃			*						*		*	
C ₂₄									*			

* For compounds marked with an asterisk, the particulate phase was quantified, but the vapour was below detection limit, and hence K_p is undefined.

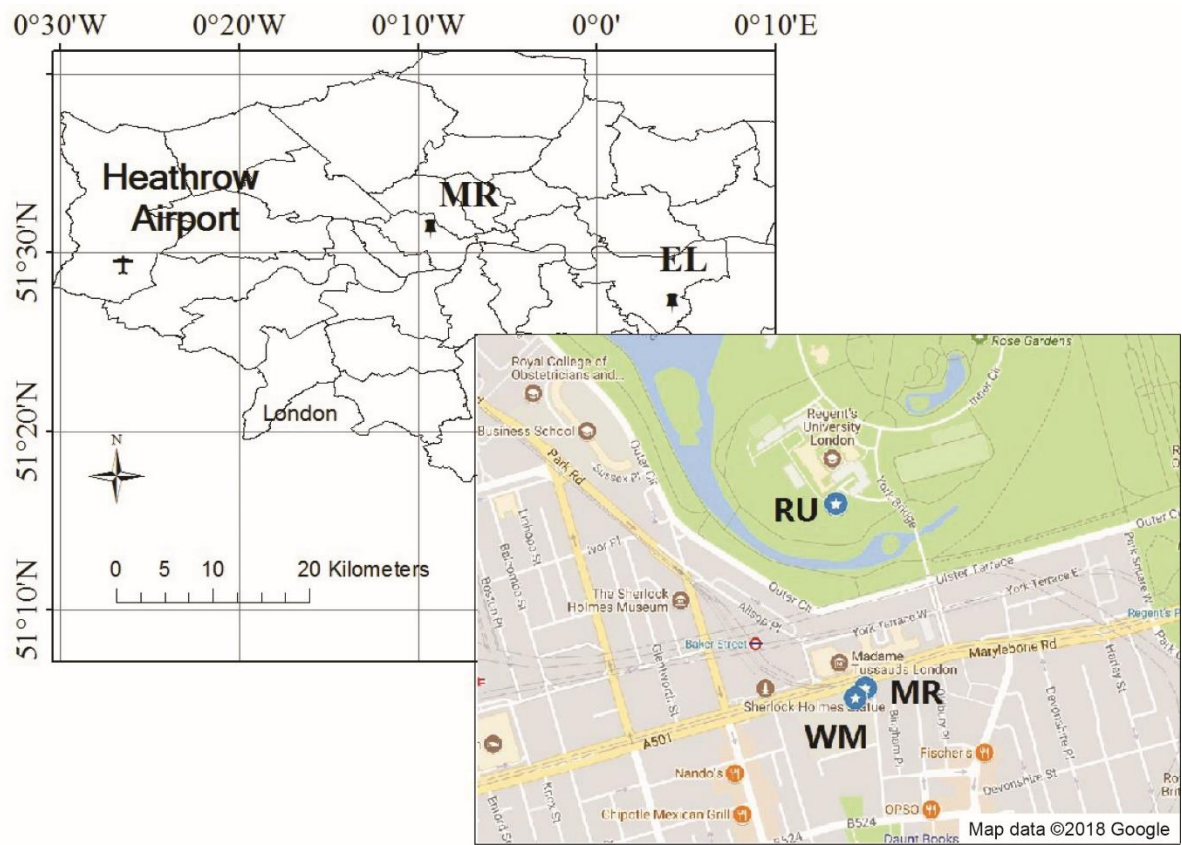


Fig. 1. Map of the sampling sites. RU-Regents University (15 m above ground); WM-University of Westminster (20 m above ground); EL-Eltham; MR-Marylebone Road (south side).

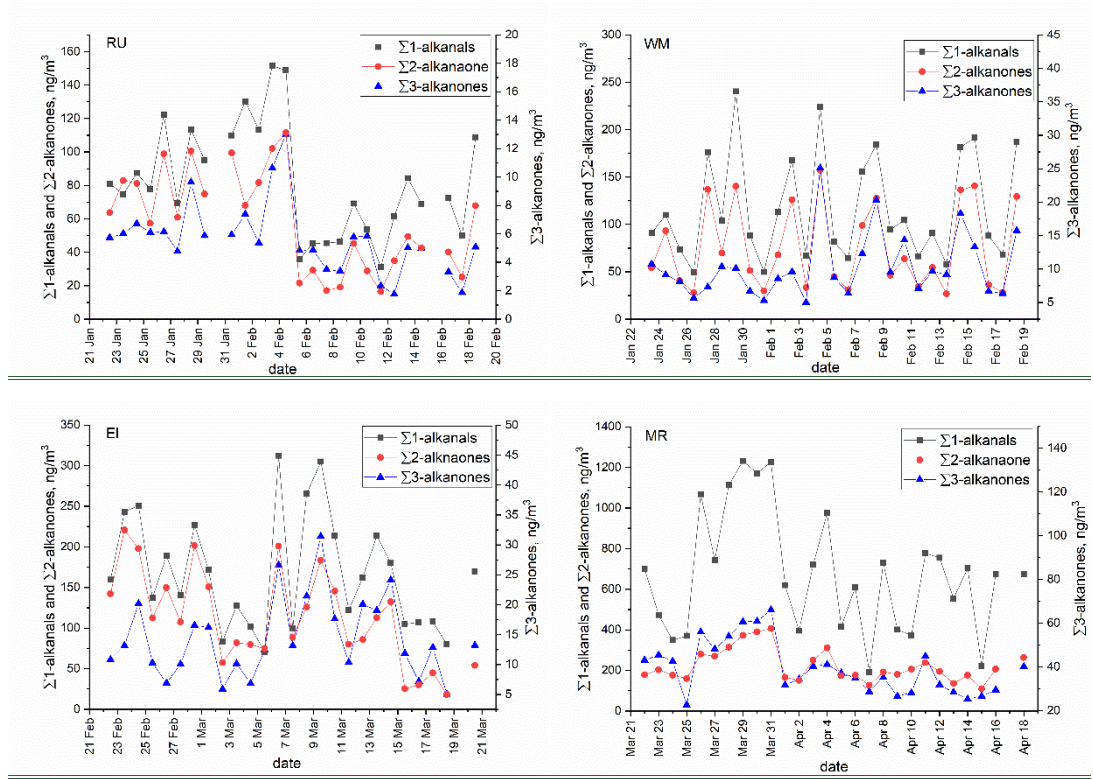


Fig. 32. Time series of particle-bound Σn -alkanals, Σn -alkan-2-ones and Σn -alkan-3-ones at RU, WM, EL, and MR sites.

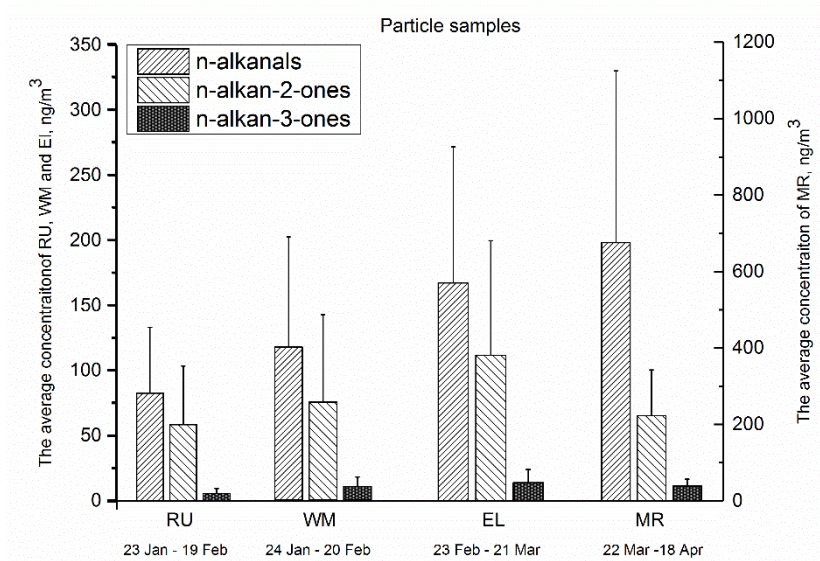


Fig. 23. The average total concentration of particle-bound n-alkanals (C_8-C_{20}), n-alkan-2-ones (C_8-C_{26}), and n-alkan-3-ones (C_8-C_{19}), for each sampling period and site. The error bars indicate one standard deviation.

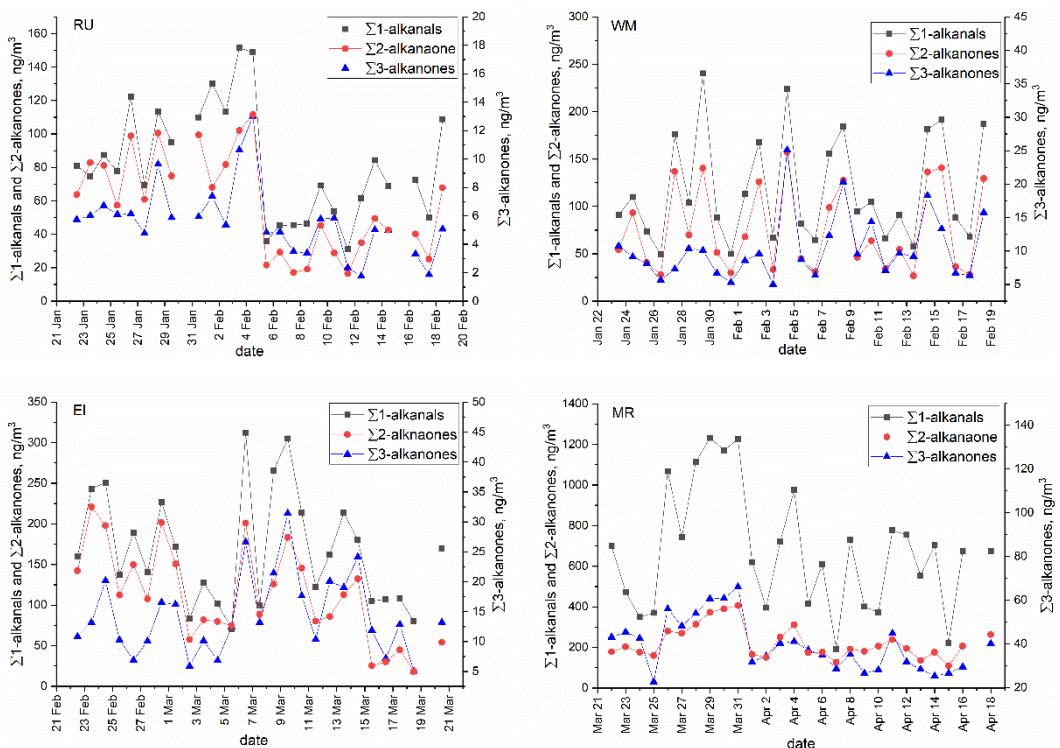


Fig. 3. Time series of particle bound Σ_1 -alkanals, Σ_2 -alkanones and Σ_3 -alkanones at RU, WM, EL, and MR sites.

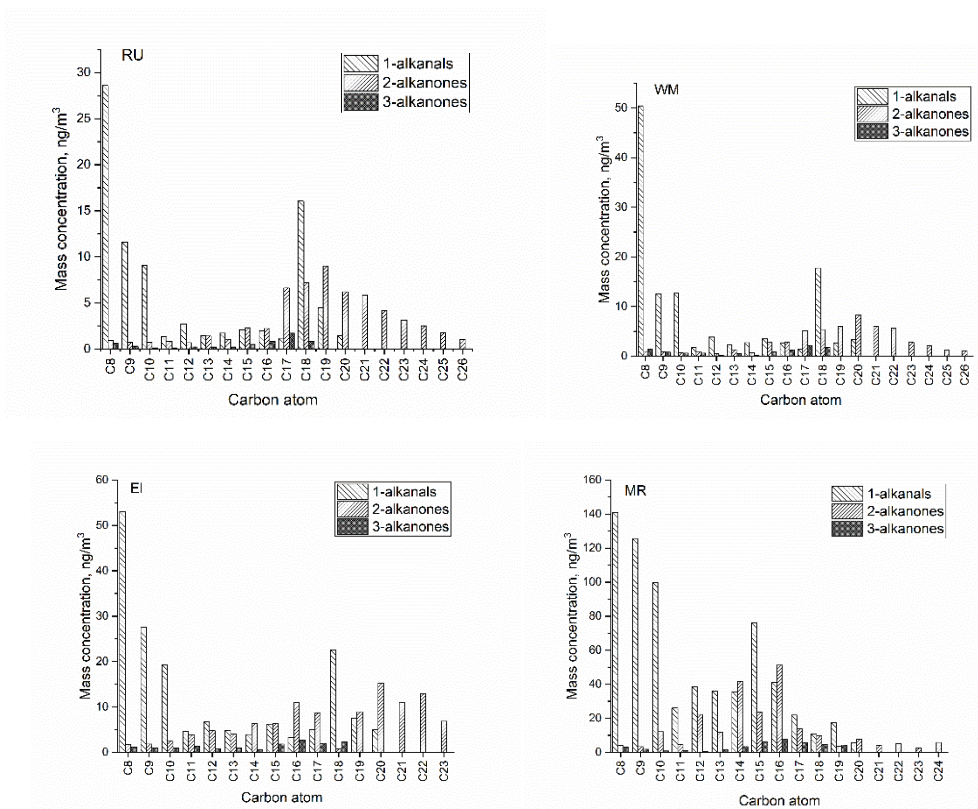


Fig. 4. The molecular distribution of particle-bound carbonyl compounds at four sites (RU, WM, EL, and MR).

1

2

3 **SUPPORTING INFORMATION**

4

5 **Aliphatic Carbonyl Compounds (C₈-C₂₆) in Wintertime Atmospheric**
6 **Aerosol in London, UK**

7

8 **Ruihe Lyu, Mohammed Salim Alam, Christopher Stark, Ruixin Xu, Zongbo**
9 **Shi, Yinchang Feng and Roy M. Harrison**

10

11

12

13

14 **Table S1:** Detection limit of gaseous (G) and particle (P) carbonyl compounds.

Carbon number	n-Alkanals	DL, ng m ⁻³		DL, ng m ⁻³		DL, ng m ⁻³			
		G	P	G	P	G	P		
C ₈	<i>n</i> -Octanal	0.013	0.008	<i>n</i> -Octan-2-one	0.015	0.011	<i>n</i> -Octan-3-one	0.010	0.008
C ₉	<i>n</i> -Nonanal	0.011	0.015	<i>n</i> -Nonan-2-one	0.010	0.008	<i>n</i> -Nonan-3-one	0.007	0.002
C ₁₀	<i>n</i> -Decanal	0.016	0.002	<i>n</i> -Decan-2-one	0.007	0.005	<i>n</i> -Decan-3-one	0.005	0.003
C ₁₁	<i>n</i> -Undecanal	0.015	0.010	<i>n</i> -Undecan-2-one	0.002	0.009	<i>n</i> -Undecan-3-one	0.005	0.003
C ₁₂	<i>n</i> -Dodecanal	0.010	0.006	<i>n</i> -Dodecan-2-one	0.005	0.001	<i>n</i> -Dodecan-3-one	0.009	0.001
C ₁₃	<i>n</i> -Tridecanal	0.010	0.009	<i>n</i> -Tridecan-2-one	0.008	0.004	<i>n</i> -Tridecan-3-one	0.008	0.002
C ₁₄	<i>n</i> -Tetradecanal	0.008	0.013	<i>n</i> -Tetradecan-2-one	0.015	0.006	<i>n</i> -Tetradecan-3-one	0.010	0.005
C ₁₅	<i>n</i> -Pentadecanal	0.015	0.005	<i>n</i> -Pentadecan-2-one	0.013	0.002	<i>n</i> -Pentadecan-3-one	0.009	0.003
C ₁₆	<i>n</i> -Hexadecanal	0.020	0.015	<i>n</i> -Hexadecan-2-one	0.006	0.001	<i>n</i> -Hexadecan-3-one	0.015	0.007
C ₁₇	<i>n</i> -Heptadecanal	0.021	0.012	<i>n</i> -Heptadecan-2-one	0.008	0.004	<i>n</i> -Heptadecan-3-one	0.009	0.004
C ₁₈	<i>n</i> -Octadecanal	0.014	0.007	<i>n</i> -Octadecan-2-one	0.011	0.012	<i>n</i> -Octadecan-3-one	0.008	0.003
C ₁₉	<i>n</i> -Nonadecanal	0.010	0.016	<i>n</i> -Nonadecan-2-one	0.020	0.006	<i>n</i> -Nonadecan-3-one	0.012	0.005
C ₂₀	<i>n</i> -Eicosanal	0.019	0.015	<i>n</i> -Eicosan-2-one	0.018	0.009			
C ₂₁				<i>n</i> -Heneicosan-2-one	0.022	0.006			
C ₂₂				<i>n</i> -Docosan-2-one	0.014	0.010			
C ₂₃				<i>n</i> -Tricosan-2-one	0.017	0.011			
C ₂₄				<i>n</i> -Tetracosan-2-one	0.010	0.015			
C ₂₅				<i>n</i> -Pentacosan-2-one	0.016	0.020			
C ₂₆				<i>n</i> -Hexacosan-2-one	0.021	0.015			

15

16

17 Table S1S2. Concentrations (ng m⁻³) in particulate (P) and gaseous (G) forms

RU (Regent University, 15 m above ground, 23 Jan - 19 Feb 2017)

	n-alkanals		n-alkanals		n-alkan-2-ones		n-alkan-2-ones		n-alkan-3-ones		n-alkan-3-ones	
	P	SD	G	SD	P	SD	G	SD	P	SD	G	SD
C ₈	28.6	10.9	5.88	3.49	0.97	0.64	4.34	1.95	0.62	0.58	1.98	1.14
C ₉	11.6	6.07	5.14	3.43	0.72	0.58	4.26	2.40	0.27	0.14	1.36	0.92
C ₁₀	9.11	5.06	2.99	2.47	0.69	0.57	4.37	2.46	0.13	0.09	1.62	1.08
C ₁₁	1.32	0.81	1.58	1.05	0.84	0.61	3.09	1.80	0.12	0.13	0.82	0.66
C ₁₂	2.73	1.50	0.92	0.59	0.67	0.54	2.01	1.47	0.26	0.39	0.57	0.45
C ₁₃	1.45	0.98	0.39	0.35	1.41	1.01	0.90	0.79	0.23	0.21	0.42	0.33
C ₁₄	1.73	1.08	0.50	0.40	1.07	0.74	1.09	0.92	0.22	0.23	0.40	0.28
C ₁₅	2.10	1.41	0.11	0.13	2.33	1.31	0.44	0.35	0.48	0.49	0.47	0.38
C ₁₆	1.98	1.21			2.23	1.35	0.21	0.18	0.85	0.60	0.36	0.20
C ₁₇	1.20	0.86			6.63	3.13	0.62	0.51	1.72	0.97		
C ₁₈	16.1	9.19			7.17	3.41	0.45	0.33	0.83	0.48		
C ₁₉	4.48	3.92			9.03	3.86						
C ₂₀	1.48	1.19			6.21	3.12						
C ₂₁					5.88	3.35						
C ₂₂					4.21	3.05						
C ₂₃					3.13	2.35						
C ₂₄					2.51	1.98						
C ₂₅					1.80	1.59						
C ₂₆					1.02	1.06						
Average	6.44	3.40	2.19	1.49	3.08	1.80	1.98	1.17	0.52	0.39	0.89	0.60

WM (Westminster University, 20 m above ground, 24 Jan - 20 Feb 2017)

	n-alkanals		n-alkanals		n-alkan-2-ones		n-alkan-2-ones		n-alkan-3-ones		n-alkan-3-ones	
	P	SD	G	SD	P	SD	G	SD	P	SD	G	SD
C ₈	50.3	18.7	12.4	4.33	0.94	0.66	6.15	2.57	1.47	1.05	2.84	1.61
C ₉	12.6	6.64	8.24	5.43	0.85	0.80	4.59	2.34	0.81	0.71	2.04	1.33
C ₁₀	12.7	6.97	2.76	1.82	0.74	0.60	4.41	2.32	0.62	0.45	2.04	1.15
C ₁₁	1.74	1.53	1.05	0.89	0.81	0.69	3.22	2.31	0.62	0.61	1.09	0.76
C ₁₂	3.87	2.92	1.38	0.81	0.57	0.54	1.41	0.87	0.20	0.19	0.68	0.56
C ₁₃	2.26	1.53	0.49	0.45	1.29	1.04	1.35	1.02	0.50	0.43	0.30	0.25
C ₁₄	2.73	1.78	0.87	0.71	0.75	0.81	1.61	0.97	0.20	0.16	0.58	0.36
C ₁₅	3.51	2.92			2.89	2.06	0.51	0.33	0.89	0.52	0.41	0.23
C ₁₆	2.62	2.02			2.84	2.15	0.33	0.29	1.21	0.64	0.11	0.17
C ₁₇	1.42	1.03			5.16	4.40	0.85	0.68	2.05	1.15	0.19	0.30
C ₁₈	17.8	11.0			5.37	4.32	0.96	0.73	1.79	1.51	0.01	0.08
C ₁₉	2.65	2.02			5.98	4.98						
C ₂₀	3.34	2.66			8.26	6.93						
C ₂₁					6.02	5.46						
C ₂₂					5.61	5.53						
C ₂₃					2.76	3.11						
C ₂₄					2.14	2.19						

C₂₅	1.17	1.18
C₂₆	1.01	1.13
Average	9.04	4.75

EL (Eltham, 23 Feb - 21 Mar 2017)

	n-alkanals		n-alkanals		n-alkan-2-ones		n-alkan-2-ones		n-alkan-3-ones		n-alkan-3-ones	
	P	SD	G	SD	P	SD	G	SD	P	SD	G	SD
C₈	53.0	22.5	4.21	1.44	1.66	0.94	5.00	2.46	1.10	0.91	2.35	1.24
C₉	27.6	21.5	2.32	4.36	1.81	1.93	2.95	1.80	0.92	0.99	4.15	0.87
C₁₀	19.3	11.6	2.02	0.96	2.56	3.28	2.82	1.66	1.01	0.79	1.14	0.66
C₁₁	4.56	4.72	0.68	0.51	3.81	4.51	1.46	0.95	1.31	1.15	0.80	0.29
C₁₂	6.75	7.02	0.52	0.49	4.76	6.24	0.95	0.73	0.73	0.95	0.37	0.27
C₁₃	4.75	3.43	0.22	0.16	5.44	6.32	0.88	0.65	0.90	0.92	0.47	0.32
C₁₄	3.94	2.43	0.37	0.36	4.07	3.30	0.68	0.53	0.52	0.54	0.36	0.30
C₁₅	6.22	4.05	0.21	0.19	6.30	4.27	0.37	0.30	1.84	1.19	0.34	0.27
C₁₆	3.29	2.92			6.41	3.28	0.40	0.28	2.66	1.69	0.33	0.24
C₁₇	5.03	4.91			10.9	5.82	0.45	0.42	1.98	1.32	0.45	0.19
C₁₈	22.6	18.3			1.56	6.16	0.45	0.31	2.26	1.48	0.40	0.57
C₁₉	7.46	4.58			11.9	11.2						
C₂₀	5.05	4.10			8.96	7.75						
C₂₁					15.2	7.22						
C₂₂					11.1	7.34						
C₂₃					13.0	9.38						
C₂₄					6.84	6.17						
Average	13.0	8.62	1.32	0.68	6.84	5.59	1.49	0.92	1.38	1.08	0.74	0.47

Formatted Table

	n-alkanals		n-alkanals		n-alkan-2-ones		n-alkan-2-ones		n-alkan-3-ones		n-alkan-3-ones	
	P	SD	G	SD	P	SD	G	SD	P	SD	G	SD
C₈	141	68.8	15.6	5.88	4.22	3.44	10.7	3.65	2.89	1.54	3.83	2.26
C₉	126	74.7	14.2	4.24	3.35	2.88	9.08	3.43	1.76	1.69	2.74	1.82
C₁₀	99.9	46.6	8.99	4.16	12.1	5.21	7.72	3.67	0.80	0.74	3.13	1.76
C₁₁	26.0	13.5	3.76	2.93	4.69	3.96	4.66	2.42	0.88	0.64	1.78	0.56
C₁₂	38.6	22.3	2.92	2.52	22.3	8.02	2.90	1.71	0.63	0.50	1.61	0.39
C₁₃	36.0	20.1	1.46	1.08	11.7	4.06	1.64	0.92	1.38	1.09	1.61	0.38
C₁₄	35.6	17.0	1.78	1.61	41.6	12.7	1.78	0.91	3.29	2.38	1.28	0.49
C₁₅	76.1	30.0			23.6	10.3	0.75	0.40	6.31	2.84	1.22	0.29
C₁₆	41.0	22.5			14.4	7.90	0.54	0.25	7.53	3.70	1.03	0.24
C₁₇	21.9	11.7			14.0	7.12	0.59	0.46	5.64	3.52	0.77	0.18
C₁₈	10.7	8.76			9.68	6.61	0.78	0.62	4.64	2.82	0.63	0.23
C₁₉	17.5	10.7			3.56	2.93			4.35	1.91		
C₂₀	5.47	4.28			7.78	6.17						
C₂₁					4.01	4.41						
C₂₂					5.12	4.40						
C₂₃					2.65	2.73						
C₂₄					5.89	4.71						
Average	13.0	8.62	1.32	0.68	6.84	5.59	1.49	0.92	1.38	1.08	0.74	0.47

Average	52.0	27.0	6.96	3.20	11.2	5.74	3.74	1.68	3.34	1.95	1.78	0.78
---------	------	------	------	------	------	------	------	------	------	------	------	------

19 Table S2S3. The ratios of n-alkan-2-ones/n-alkanes, and n-alkan-3-ones/n-alkanes with same
 20 carbon numbers.

Carbon numbers	n-alkan-2-ones/n-alkanes, %				
	RU	WM	EL	MR	
				Northerly winds	Southerly winds
C13	2.31	1.86	2.14	6.02	6.34
C14	2.03	1.58	2.38	20.8	15.9
C15	4.17	4.77	5.95	11.3	13.6
C16	7.35	5.98	8.58	11.8	7.27
C17	48.9	29.8	31.7	27.0	24.6
C18	32.5	18.2	31.3	23.4	18.1
C19	77.8	33.9	43.2	19.6	14.7
C20	379	168	33.3	32.8	10.1
C21	267	59.3	33.1	10.4	3.18
C22	144	36.1	18.6	4.76	5.29
C23	17.1	6.61	10.5	1.75	3.41
C24	17.1	7.16	11.3	3.31	5.62
C25	26.5	4.24			
C26	18.3	3.36			
averages	74.7	27.2	19.3	14.4	10.1
min	2.03	1.58	2.14	1.75	3.18
max	379	168	43.2	32.8	24.6

21

Carbon numbers	n-alkan-3-ones/n-alkanes, %				
	RU	WM	EL	MR	
				Northerly winds	Southerly winds
C13	0.70	0.50	0.49	1.30	1.39
C14	0.58	0.50	0.47	2.10	1.73
C15	1.31	1.51	2.15	5.22	3.58
C16	3.80	1.73	3.87	14.9	4.44
C17	12.4	7.17	8.39	15.7	8.58
C18	3.78	3.87	7.61	11.1	3.59
C19				7.65	8.27
averages	3.76	2.55	3.83	8.28	4.51
min	0.58	0.50	0.47	1.30	1.39
max	12.4	7.17	8.39	15.7	8.58

22

23

24

25

26 Table S3S4. The regression equations between black carbon (BC) and n-alkanals, NO_x and n-
 27 alkanals.

28
 29 C_n-alkanals = m C_{BC} + b

Carbon atoms	RU			WM			MR					
	m	b	r ²	m	b	r ²	Northerly Winds			Southerly winds		
							m	b	r ²	m	b	r ²
C8	-0.43	34.3	0.00	-5.30	73.5	0.03	40.5	30.7	0.27	39.6	17.5	0.49
C9	3.88	21.2	0.06	-0.63	21.5	0.00	18.6	71.2	0.09	57.0	108	0.61
C10	-2.00	14.5	0.02	-1.55	18.3	0.02	4.39	95.7	0.05	36.2	-48.8	0.53
C11	0.11	2.28	0.00	-0.18	3.25	0.01	-0.33	27.4	0.02	12.6	-25.2	0.57
C12	-1.25	5.23	0.11	-0.17	5.84	0.00	2.17	30.1	0.02	20.7	-47.3	0.56
C13	-0.10	1.87	0.00	0.01	2.84	0.00	-4.36	46.7	0.09	12.6	-12.7	0.58
C14	-0.23	2.48	0.02	0.11	3.60	0.00	6.37	19.5	0.18	9.57	-0.65	0.49
C15	-0.33	2.57	0.01	-0.69	5.25	0.02	6.59	57.0	0.12	18.3	5.08	0.43
C16	0.85	0.81	0.09	-0.01	2.75	0.00	5.57	29.6	0.08	8.18	9.85	0.28
C17	-0.35	1.66	0.04	0.05	1.33	0.00	4.73	4.67	0.31	5.79	0.94	0.35
C18	-6.42	25.2	0.10	-1.90	21.7	0.01	0.81	6.19	0.03	8.61	-26.2	0.44
C19	-2.80	7.88	0.15	-0.35	3.38	0.01	3.74	4.81	0.50	7.08	-9.39	0.38
C20	0.11	1.33	0.00	-1.04	5.44	0.07	0.79	2.18	0.14	2.38	-3.11	0.34
Average			0.05			0.01			0.15			0.47
Min	-6.42	0.81	0.00	-5.30	1.33	0.00	-4.36	2.18	0.02	2.38	-108	0.28
Max	0.85	34.3	0.15	0.11	73.5	0.07	40.5	95.7	0.50	57.02	17.5	0.61

30 Formatted Table

31 C_n-alkanals = m C_{NOx} + b

Carbon atoms	EL			MR					
	m	b	r ²	Northerly Winds			Southerly winds		
				m	b	r ²	m	b	r ²
C8	-0.75	72.9	0.12	0.67	27.4	0.21	0.53	32.8	0.50
C9	1.05	4.38	0.31	0.38	54.4	0.06	0.56	-5.49	0.48
C10	0.44	10.4	0.16	0.11	83.2	0.01	0.36	13.0	0.42
C11	0.16	1.48	0.13	0.01	25.6	0.01	0.11	1.73	0.49
C12	0.06	5.51	0.01	0.14	13.1	0.19	0.18	-2.49	0.45
C13	0.08	2.92	0.07	-0.02	35.3	0.01	0.14	1.35	0.38
C14	0.03	3.59	0.02	0.15	12.1	0.23	0.13	4.64	0.35
C15	0.00	6.14	0.00	0.20	39.9	0.15	0.14	47.4	0.15
C16	0.07	1.72	0.07	0.18	17.0	0.20	0.11	11.0	0.12
C17	-0.09	7.04	0.05	0.08	4.19	0.28	0.05	11.4	0.11
C18	-0.49	34.1	0.09	0.02	5.64	0.03	0.07	-8.65	0.30
C19	0.05	6.24	0.02	3.74	4.81	0.50	0.07	1.14	0.23
C20	-0.06	6.33	0.03	0.00	3.28	0.01	0.03	-2.08	0.24
Average			0.08			0.15			0.32
Min	-0.75	1.48	0.00	-0.02	3.28	0.01	0.03	-8.65	0.11
Max	1.05	72.9	0.31	3.74	83.2	0.50	0.56	47.4	0.50

32 Formatted Table

34 Table S5. Concentrations of PM₁₀ at the sampling sites.

35

<u>Sites</u>	<u>PM₁₀ Range, µg/m³</u>	<u>PM₁₀ Mean µg/m³</u>	<u>Note</u>
<u>RU and WM</u>	<u>10.8-72.4</u>	<u>34.1</u>	<u>The sampling period was dominated by southerly winds and the data from London, North Kensington were used as this is an upwind urban background site.</u>
<u>EL</u>	<u>4.37-27.1</u>	<u>19.3</u>	<u>The PM₁₀ data was obtained from the London North Kensington site (Defra), because the EL only have PM_{2.5} data, and the PM_{2.5} data of two site (EL and London North Kensington) were close to each other.</u>
<u>MR</u>	<u>12.6-78.7</u>	<u>30.7</u>	<u>MR site</u>

36

37

38
39

Table S4S6. Analysis of n-alkanals, alkan-2-ones and alkan-3-ones partitioning, all compounds, daily data at RU, WM, El and MR sites.

Formatted: No Spacing

Date	Temp °C	RU											
		alkanals (C ₁₀ -C ₁₄)			alkan-2-ones(C ₁₀ -C ₁₈)			alkan-3-ones(C ₁₀ -C ₁₆)			All Carbonyl compounds		
		m	b	r ²		m	b	r ²		m	b	r ²	
26/01/2017	0.41	-0.22	-1.73	0.09	-0.55	-4.67	0.50	-0.12	-2.27	0.15	-0.25	-2.80	0.11
27/01/2017	7.17	-0.24	-1.71	0.18	-0.40	-3.33	0.83	-0.24	-3.19	0.26	-0.26	-2.58	0.19
28/01/2017	5.44	-0.29	-1.76	0.15	-0.47	-3.48	0.88	-0.28	-2.82	0.53	-0.31	-2.54	0.34
29/01/2017	8.28	-0.30	-1.49	0.18	-0.43	-2.86	0.81	-0.24	-2.16	0.42	-0.33	-2.20	0.41
03/02/2017	5.58	-0.18	-1.68	0.02	-0.41	-3.42	0.87	-0.43	-3.80	0.90	-0.36	-3.08	0.45
04/02/2017	5.15	-0.34	-2.44	0.64	-0.40	-3.37	0.95	-0.29	-3.18	0.59	-0.33	-2.93	0.55
05/02/2017	3.70	-0.27	-2.25	0.37	-0.35	-3.30	0.84	-0.34	-3.54	0.62	-0.29	-2.90	0.50
06/02/2017	6.30	-0.08	-1.88	0.05	-0.41	-4.21	0.92	-0.44	-4.48	0.47	-0.34	-3.67	0.53
07/02/2017	5.60	-0.03	-1.90	0.02	-0.48	-4.96	0.83	-0.58	-5.54	0.58	-0.41	-4.38	0.57
08/02/2017	2.84	-0.10	-0.74	0.17	-0.54	-5.51	0.90	-0.34	-3.83	0.61	-0.34	-3.77	0.48
09/02/2017	1.65	-0.16	-2.30	0.15	-0.49	-5.27	0.95	-0.24	-3.67	0.39	-0.31	-3.86	0.47
10/02/2017	1.38	-0.14	-1.71	0.07	-0.46	-4.48	0.93	-0.42	-4.47	0.47	-0.35	-3.61	0.44
11/02/2017	2.30	-0.14	-1.86	0.21	-0.49	-5.02	0.87	-0.37	-4.34	0.84	-0.33	-3.74	0.45
12/02/2017	5.67	-0.08	-1.38	0.04	-0.54	-5.55	0.89	-0.35	-4.59	0.67	-0.38	-4.41	0.55
13/02/2017	5.60	-0.10	-1.11	0.13	-0.48	-5.07	0.92	-0.48	-5.18	0.85	-0.36	-4.25	0.53
14/02/2017	9.51	-0.48	-3.83	0.62	-0.42	-4.43	0.94	-0.37	-4.51	0.89	-0.34	-3.87	0.51
15/02/2017	7.96	-0.10	-1.43	0.33	-0.51	-4.53	0.89	-0.50	-4.65	0.62	-0.40	-3.69	0.54
17/02/2017	7.83	-0.20	-2.42	0.40	-0.46	-4.80	0.94	-0.23	-3.69	0.48	-0.30	-3.63	0.43
18/02/2017	7.72	-0.14	-2.20	0.12	-0.56	-5.47	0.91	-0.48	-5.17	0.77	-0.42	-4.42	0.57
19/02/2017	11.38	-0.31	-2.35	0.63	-0.37	-3.72	0.92	-0.42	-4.40	0.78	-0.30	-5.20	0.42
Average	5.57	-0.20	-1.91	0.23	-0.46	-4.37	0.87	-0.36	-3.97	0.59	-0.34	-3.58	0.45
MIN		-0.48	-3.83	0.02	-0.56	-5.55	0.50	-0.58	-5.54	0.15	-0.42	-5.20	0.11

Date	Temp	alkanals (C ₁₀ -C ₁₄)			alkan-2-ones(C ₁₀ -C ₁₈)			alkan-3-ones(C ₁₀ -C ₁₆)			All Carbonyl compounds		
		°C	m	b	r ²	m	b	r ²	m	b	r ²	m	b
	MAX	-0.03	-0.74	0.64	-0.35	-2.86	0.95	-0.12	-2.16	0.90	-0.25	-2.20	0.57

RU

Date	Temp	alkanals (C ₁₀ -C ₁₄)			alkan-2-ones(C ₁₀ -C ₁₈)			alkan-3-ones(C ₁₀ -C ₁₆)			All Carbonyl compounds		
		°C	m	b	r ²	m	b	r ²	m	b	r ²	m	b
	26/01/2017	0.41	-0.34	0.46	0.97	-0.41	-4.36	0.73	-0.39	-4.60	0.55	-0.24	-3.29
27/01/2017	7.17	-0.17	-1.95	0.20	-0.59	-5.44	0.93	-0.54	-4.96	0.63	-0.43	-4.08	0.49
28/01/2017	5.44	-0.15	-1.32	0.31	-0.35	-2.90	0.88	-0.44	-3.42	0.84	-0.32	-2.55	0.66
29/01/2017	8.28	-0.15	-1.35	0.35	-0.30	-2.63	0.58	-0.42	-3.45	0.40	-0.22	-1.99	0.22
03/02/2017	5.58	-0.14	-1.11	0.31	-0.46	-3.05	0.90	-0.19	-2.26	0.22	-0.34	-2.29	0.33
04/02/2017	5.15	-0.06	-1.12	0.11	-0.44	-3.87	0.87	-0.03	-1.07	0.43	-0.24	-2.35	0.25
05/02/2017	3.70	-0.06	-1.24	0.14	-0.36	-2.77	0.87	-0.09	-1.72	0.17	-0.24	-2.03	0.31
06/02/2017	6.30	-0.04	-1.02	0.11	-0.33	-3.02	0.51	-0.14	-0.51	0.21	-0.14	-1.70	0.19
07/02/2017	5.60	-0.08	-1.85	0.09	-0.43	-4.68	0.86	-0.21	-3.15	0.32	-0.27	-3.37	0.43
08/02/2017	2.84	-0.27	-2.47	0.29	-0.44	-4.17	0.91	-0.56	-5.16	0.92	-0.39	-3.79	0.64
09/02/2017	1.65	-0.12	-1.30	0.16	-0.39	-3.48	0.92	-0.29	-3.09	0.24	-0.31	-2.85	0.47
10/02/2017	1.38	-0.20	-2.03	0.53	-0.42	-4.23	0.95	-0.28	-3.34	0.46	-0.30	-3.21	0.54
11/02/2017	2.30	-0.01	-1.33	0.28	-0.44	-4.55	0.89	-0.16	-2.37	0.35	-0.27	-3.10	0.49
12/02/2017	5.67	-0.24	-2.61	0.17	-0.44	-4.65	0.88	-0.42	-4.77	0.55	-0.34	-3.89	0.43
13/02/2017	5.60	-0.05	-1.12	0.11	-0.43	-4.44	0.88	-0.33	-3.99	0.52	-0.31	-3.58	0.48
14/02/2017	9.51	-0.03	-1.66	0.09	-0.38	-4.61	0.88	-0.11	-2.61	0.23	-0.21	-3.23	0.35
15/02/2017	7.96	-0.07	-1.17	0.12	-0.36	-3.24	0.93	-0.53	-4.47	0.77	-0.33	-3.00	0.54
16/02/2017	9.27	-0.35	-2.66	0.40	-0.35	-3.40	0.85	-0.39	-3.81	0.78	-0.30	-2.96	0.51

Date	Temp	alkanals (C ₁₀ -C ₁₄)			alkan-2-ones(C ₁₀ -C ₁₈)			alkan-3-ones(C ₁₀ -C ₁₆)			All Carbonyl compounds		
		°C	m	b	r ²	m	b	r ²	m	b	r ²	m	b
17/02/2017	7.83	-0.25	-2.43	0.23	-0.35	-3.99	0.86	-0.40	-4.51	0.51	-0.28	-3.34	0.33
18/02/2017	7.72	-0.30	-2.96	0.26	-0.37	-4.30	0.85	-0.35	-4.01	0.61	-0.28	-3.44	0.43
19/02/2017	11.38	-0.22	-1.24	0.21	-0.51	-4.11	0.88	-0.48	-3.82	0.81	-0.40	-3.24	0.61
Average	6.02	-0.16	-1.59	0.26	-0.41	-3.90	0.85	-0.32	-3.39	0.50	-0.29	-3.01	0.42
MIN		-0.35	-2.96	0.09	-0.59	-5.44	0.51	-0.56	-5.16	0.17	-0.43	-4.08	0.19
MAX		-0.01	0.46	0.97	-0.30	-2.63	0.95	-0.03	-0.51	0.92	-0.14	-1.70	0.66

Date	Temp	alkanals (C ₁₀ -C ₁₄)			alkan-2-ones(C ₁₀ -C ₁₈)			alkan-3-ones(C ₁₀ -C ₁₆)			All Carbonyl compounds		
		°C	m	b	r ²	m	b	r ²	m	b	r ²	m	b
23/02/2017	5.20	-0.13	-0.59	0.16	-0.34	-2.45	0.72	-0.32	-2.62	0.53	-0.26	-1.89	0.39
24/02/2017	5.58	-0.05	-0.78	0.11	-0.39	-3.03	0.77	-0.39	-3.07	0.76	-0.28	-2.14	0.43
25/02/2017	9.36	-0.01	-0.82	0.09	-0.29	-1.40	0.60	-0.22	-1.2	0.10	-0.19	-0.66	0.16
26/02/2017	9.82	-0.07	-0.26	0.05	-0.37	-2.48	0.85	-0.26	-1.69	0.24	-0.27	-1.66	0.44
27/02/2017	4.16	-0.07	-0.16	0.08	-0.54	-3.71	0.90	-0.22	-1.48	0.01	-0.30	-2.04	0.35
28/02/2017	5.55	-0.32	-2.40	0.42	-0.53	-4.6	0.94	-0.11	-1.82	0.14	-0.32	-2.99	0.49
01/03/2017	6.57	-0.26	-1.50	0.69	-0.48	-3.68	0.87	-0.37	-5.07	0.71	-0.36	-2.71	0.57
02/03/2017	5.77	-0.21	-1.61	0.56	-0.48	-3.47	0.91	-0.34	-2.81	0.46	-0.40	-2.90	0.69
03/03/2017	8.09	-0.16	0.55	0.64	-0.17	-2.13	0.46	-0.13	-2.61	0.08	-0.10	-1.81	0.06
04/03/2017	6.98	-0.09	-0.32	0.16	-0.32	-2.65	0.77	-0.15	-1.24	0.12	-0.11	-1.17	0.10
05/03/2017	6.19	-0.24	-1.27	0.35	-0.45	-3.25	0.9	-0.05	-0.90	0.04	-0.27	-1.96	0.42
06/03/2017	5.13	-0.13	-1.18	0.19	-0.37	-3.28	0.71	-0.17	-1.86	0.20	-0.24	-2.18	0.37
07/03/2017	8.12	-0.16	-0.33	0.21	-0.28	-1.97	0.71	-0.22	-1.7	0.21	-0.17	-1.07	0.17

42

43

Date	Temp	alkanals (C ₁₀ -C ₁₄)			alkan-2-ones(C ₁₀ -C ₁₈)			alkan-3-ones(C ₁₀ -C ₁₆)			All Carbonyl compounds		
		°C	m	b	r ²	m	b	r ²	m	b	r ²	m	b
	08/03/2017	9.89	-0.05	-0.74	0.03	-0.41	-3.40	0.84	-0.28	-2.58	0.31	-0.29	-2.45
09/03/2017	6.83	-0.09	-0.39	0.70	-0.21	-1.73	0.53	-0.18	-1.98	0.19	-0.14	-1.28	0.14
10/03/2017	7.69	-0.01	-0.79	0.33	-0.12	-1.32	0.37	-0.19	-2.05	0.61	-0.09	-1.11	0.10
11/03/2017	7.12	-0.32	-1.74	0.35	-0.12	-1.16	0.33	-0.21	-2.17	0.18	-0.14	-1.27	0.13
12/03/2017	7.50	-0.23	-1.19	0.79	-0.10	-0.63	0.16	-0.30	-2.49	0.22	-0.09	-0.93	0.03
13/03/2017	8.21	-0.06	0.20	0.01	-0.30	-1.94	0.84	-0.19	-1.79	0.23	-0.22	-1.37	0.23
14/03/2017	7.88	-0.11	1.25	0.10	-0.08	-0.81	0.12	-0.25	-2.20	0.28	-0.07	-0.74	0.04
15/03/2017	8.04	-0.14	-1.07	0.21	-0.18	-1.43	0.54	-0.34	-2.84	0.45	-0.21	-1.72	0.35
16/03/2017	7.37	-0.16	-1.04	0.07	-0.38	-3.56	0.54	-0.13	-1.88	0.12	-0.19	-2.01	0.14
17/03/2017	10.23	-0.50	-1.96	0.77	-0.21	-1.93	0.37	-0.11	-1.39	0.07	-0.12	-1.05	0.05
18/03/2017	11.11	-0.35	-1.97	0.24	-0.30	-2.79	0.49	-0.74	-5.47	0.83	-0.27	-2.40	0.25
19/03/2017	11.14	-0.28	-1.08	0.38	-0.19	-1.76	0.60	-0.11	-1.49	0.04	-0.08	-0.87	0.03
21/03/2017	6.53	-0.19	-0.64	0.89	-0.17	-1.12	0.55	-0.06	-0.91	0.01	-0.09	-0.59	0.05
Average	7.82	-0.17	-0.84	0.33	-0.30	-2.37	0.63	-0.23	-2.20	0.27	-0.20	-1.65	0.25
MIN		-0.50	-2.40	0.01	-0.54	-4.60	0.12	-0.74	-5.47	0.01	-0.40	-2.99	0.03
MAX		-0.01	1.25	0.89	-0.08	-0.63	0.94	-0.05	-0.90	0.83	-0.07	-0.59	0.69

Date	Temp	alkanals (C ₁₀ -C ₁₄)			alkan-2-ones(C ₁₀ -C ₁₈)			alkan-3-ones(C ₁₀ -C ₁₆)			All Carbonyl compounds		
		°C	m	b	r ²	m	b	r ²	m	b	r ²	m	b
	22/03/2017	8.01	-0.32	-1.47	0.88	-0.16	-1.24	0.18	-0.66	-5.40	0.76	-0.25	-2.03
23/03/2017	8.64	-0.38	-1.76	0.57	-0.29	-2.48	0.45	-0.40	-3.94	0.87	-0.23	-2.07	0.13

MR													
Date	Temp	alkanals (C ₁₀ -C ₁₄)			alkan-2-ones(C ₁₀ -C ₁₈)			alkan-3-ones(C ₁₀ -C ₁₆)			All Carbonyl compounds		
		°C	m	b	r ²	m	b	r ²	m	b	r ²	m	b
24/03/2017	9.01	-0.25	-1.86	0.81	-0.29	-2.71	0.45	-0.37	-3.69	0.80	-0.26	-2.56	0.34
25/03/2017	10.08	-0.47	-2.77	0.57	-0.31	-2.48	0.56	-0.45	-4.26	0.88	-0.32	-2.73	0.33
26/03/2017	9.95	-0.15	-1.31	0.33	-0.30	-2.36	0.61	-0.62	-5.11	0.78	-0.31	-2.51	0.28
27/03/2017	10.47	-0.17	-1.89	0.21	-0.41	-3.56	0.77	-0.39	-3.98	0.60	-0.38	-3.45	0.58
28/03/2017	13.05	-0.18	-0.84	0.58	-0.34	-2.20	0.68	-0.42	-3.66	0.80	-0.34	-2.35	0.36
29/03/2017	13.74	-0.45	-2.07	0.65	-0.23	-1.73	0.40	-0.28	-2.77	0.72	-0.23	-1.78	0.20
30/03/2017	15.45	-0.28	-1.76	0.69	-0.29	-2.29	0.65	-0.65	-4.92	0.85	-0.34	-2.65	0.44
31/03/2017	11.94	-0.59	-3.05	0.81	-0.28	-2.15	0.83	-0.30	-3.0	0.79	-0.27	-2.15	0.33
01/04/2017	10.82	-0.23	-1.50	0.45	-0.17	-1.86	0.26	-0.61	-5.32	0.84	-0.23	-2.35	0.17
02/04/2017	11.08	-0.35	-2.55	0.77	-0.29	-2.59	0.6	-0.35	-3.85	0.47	-0.29	-2.82	0.34
03/04/2017	12.29	-0.23	-1.71	0.39	-0.14	-1.45	0.20	-0.33	-3.43	0.79	-0.19	-2.01	0.2
04/04/2017	10.76	-0.17	-0.77	0.15	-0.26	-1.79	0.49	-0.30	-2.83	0.84	-0.23	-1.72	0.23
05/04/2017	10.83	-0.43	-2.20	0.91	-0.16	-1.20	0.22	-0.36	-3.61	0.78	-0.21	-1.85	0.15
06/04/2017	12.00	-0.14	-0.90	0.40	-0.36	-2.64	0.63	-0.32	-3.19	0.61	-0.22	-2.08	0.24
07/04/2017	12.38	-0.32	-3.09	0.90	-0.25	-2.81	0.59	-0.43	-5.03	0.29	-0.31	-3.54	0.27
08/04/2017	15.34	-0.17	-1.58	0.07	-0.29	-2.91	0.47	-0.33	-3.68	0.59	-0.23	-2.65	0.23
09/04/2017	15.11	-0.18	-1.58	0.19	-0.19	-1.84	0.37	-0.65	-5.45	0.91	-0.30	-2.73	0.31
10/04/2017	10.42	-0.16	-1.02	0.23	-0.26	-1.67	0.65	-0.52	-4.56	0.94	-0.33	-2.51	0.33
11/04/2017	11.30	-0.15	-1.31	0.51	-0.27	-2.32	0.57	-0.58	-4.99	0.87	-0.32	-2.77	0.38
12/04/2017	11.75	-0.11	-0.69	0.28	-0.35	-2.37	0.58	-0.34	-3.19	0.84	-0.27	-2.05	0.25
13/04/2017	11.20	-0.02	-0.29	0.03	-0.24	-2.04	0.56	-0.50	-4.52	0.78	-0.24	-2.23	0.22
14/04/2017	11.96	-0.11	-0.57	0.2	-0.31	-2.63	0.68	-0.28	-3.07	0.66	-0.23	-2.17	0.27
15/04/2017	10.68	-0.14	-0.72	0.15	-0.24	-1.83	0.22	-0.43	-4.08	0.44	-0.25	-2.11	0.14

44

45

46

Date	Temp	MR											
		alkanals (C ₁₀ -C ₁₄)			alkan-2-ones(C ₁₀ -C ₁₈)			alkan-3-ones(C ₁₀ -C ₁₆)			All Carbonyl compounds		
		°C	m	b	r ²	m	b	r ²	m	b	r ²	m	b
16/04/2017	10.96	-0.02	0.44	0.02	-0.17	-0.90	0.23	-0.36	-3.42	0.68	-0.20	-1.44	0.12
18/04/2017	9.01	-0.13	-0.58	0.04	-0.30	-2.03	0.67	-0.37	-3.34	0.92	-0.27	-2.03	0.29
Average	11.95	-0.23	-1.46	0.44	-0.26	-2.15	0.50	-0.43	-4.01	0.74	-0.27	-2.35	0.27
MIN		-0.59	-3.09	0.02	-0.41	-3.56	0.18	-0.66	-5.45	0.29	-0.38	-3.54	0.12
MAX		-0.02	0.44	0.91	-0.14	-0.90	0.83	-0.28	-2.77	0.94	-0.19	-1.44	0.58

Date	Temp	RU												
		°C	m	b	r ²	m	b	r ²	m	b	r ²	m	b	r ²
26/01/2017	0.44	-0.29	-5.61	0.16	-1.04	-7.45	0.49	-0.47	-6.56	0.14				
27/01/2017	7.17	-0.73	-5.41	0.26	-1.78	-7.59	0.87	-1.24	-8.36	0.18				
28/01/2017	5.44	-0.68	5.13	0.26	-1.86	6.97	0.78	-1.78	-8.17	0.48				
29/01/2017	8.28	-0.25	-5.09	0.20	-1.79	-6.44	0.75	-1.42	-6.95	0.27				
03/02/2017	5.58	0.06	-5.23	0.07	-1.94	-7.91	0.67	-2.04	-8.28	0.73				
04/02/2017	5.15	-2.07	-6.38	0.52	-1.95	-7.94	0.83	-2.14	-8.92	0.43				
05/02/2017	3.70	-1.28	-6.27	0.23	-2.22	-8.60	0.78	-1.82	-8.57	0.56				
06/02/2017	6.30	0.72	-4.22	0.12	-2.08	9.30	0.78	-1.18	-7.90	0.44				
07/02/2017	5.60	1.42	-2.96	0.27	-1.77	-9.30	0.72	-1.01	-7.89	0.29				
08/02/2017	2.84	2.64	-2.21	0.63	-1.52	-9.09	0.60	-1.87	-9.34	0.59				
09/02/2017	4.65	-1.06	-6.81	0.18	-1.93	-9.94	0.81	-1.58	-9.73	0.35				
10/02/2017	4.38	0.12	-5.39	0.20	-1.83	-8.76	0.54	-0.74	-7.17	0.04				
11/02/2017	2.30	-1.29	-6.78	0.13	-1.76	-9.26	0.77	-1.09	-8.25	0.12				
12/02/2017	5.67	1.41	-2.87	0.37	-1.54	-9.40	0.66	-1.66	-10.01	0.34				
13/02/2017	5.60	1.69	-2.26	0.41	-1.74	-9.80	0.72	-1.77	-10.62	0.54				
14/02/2017	9.51	-0.83	-6.06	0.16	-2.08	-9.62	0.76	-1.06	-8.23	0.12				
15/02/2017	7.96	1.24	-4.06	0.12	-1.65	-8.15	0.78	-1.01	-7.04	0.07				
17/02/2017	7.83	0.13	-4.72	0.18	-1.95	-9.61	0.73	-1.72	-9.89	0.19				
18/02/2017	7.72	0.66	-4.07	0.15	-1.50	-8.92	0.73	-1.02	-8.20	0.30				
19/02/2017	11.4	-0.35	-5.04	0.04	-2.33	-9.03	0.64	-0.98	-7.47	0.10				

Average			0.23			0.72			0.31
Min	-1.29			-2.33			-1.87		
Max	2.64			-1.50			-0.74		

WM

Date	Temp	alkanals (C ₈ -C ₁₄)				alkan-2-ones (C ₈ -C ₁₆)				alkan-3-ones (C ₈ -C ₁₆)			
		°C	m	b	r ²	m	b	r ²	m	b	r ²		
26/01/2017	0.41	-1.26	-1.79	0.52	-1.83	-9.55	0.71	-1.29	8.44	0.35			
27/01/2017	7.17	-1.14	-6.34	0.28	-1.51	-8.48	0.77	-0.65	7.11	0.31			
28/01/2017	5.44	-0.84	-5.84	0.20	-2.29	-7.71	0.86	-1.72	7.40	0.34			
29/01/2017	8.28	-2.49	-6.57	0.28	-2.02	-7.70	0.57	-0.74	6.60	0.31			
03/02/2017	5.58	-0.84	-5.11	0.09	-1.76	6.14	0.70	-1.20	6.77	0.31			
04/02/2017	5.15	-2.55	-6.46	0.37	-1.75	-6.43	0.79	-0.55	6.24	0.11			
05/02/2017	3.70	-1.76	-5.83	0.46	-2.16	-7.38	0.82	-1.56	7.42	0.35			
06/02/2017	6.30	-0.45	-5.37	0.07	-1.69	-7.83	0.55	1.00	4.13	0.22			
07/02/2017	5.60	0.08	-5.03	0.23	-2.06	-9.83	0.75	-1.73	9.16	0.60			
08/02/2017	2.84	-1.16	-6.47	0.21	-1.86	-8.79	0.77	-1.36	8.29	0.81			
09/02/2017	1.65	-1.84	-6.55	0.38	-2.28	-8.36	0.87	-0.84	7.15	0.39			
10/02/2017	1.38	-2.02	-7.49	0.39	-1.96	-9.24	0.74	-1.10	7.43	0.37			
11/02/2017	2.30	-0.76	-6.44	0.06	-2.02	-9.50	0.83	-2.06	8.77	0.34			
12/02/2017	5.67	-0.90	-6.31	0.18	-1.86	-9.61	0.84	-0.62	7.27	0.14			
13/02/2017	5.60	0.39	-4.44	0.17	-1.87	-9.50	0.77	-0.94	7.81	0.24			
14/02/2017	9.51	1.34	-2.41	0.22	-2.20	-10.8	0.74	-0.35	6.50	0.19			
15/02/2017	7.96	0.52	-4.72	0.08	-2.37	-8.47	0.87	-1.17	6.94	0.52			
16/02/2017	9.27	-0.75	-5.49	0.23	-2.35	-8.83	0.66	-1.67	8.25	0.52			
17/02/2017	7.83	-0.88	-5.97	0.17	-2.26	-10.1	0.82	-0.96	7.87	0.42			
18/02/2017	7.72	-0.64	-5.77	0.06	-1.87	-9.82	0.77	-1.46	8.66	0.42			
19/02/2017	11.4	1.41	-3.66	0.50	-1.61	-7.61	0.75	-1.71	7.43	0.55			
Average				0.24			0.76			0.40			
Min	-2.55				-2.37			-2.06					
Max	1.41				-1.61			1.00					

49 **Table S5.** Concentrations of PM_{10} at the sampling sites.

50

Sites	PM ₁₀ Range, $\mu\text{g}/\text{m}^3$	PM ₁₀ Mean, $\mu\text{g}/\text{m}^3$	Note
RU and WM	10.8-72.4	34.1	The sampling period was dominated by southerly winds and the data from London, North Kensington were used as this is an upwind urban background site.
EL	4.37-27.1	19.3	The PM ₁₀ data was obtained from the London North Kensington site (Defra), because the EL only have PM _{2.5} data and the PM _{2.5} data of two site (EL and London North Kensington) were close to each other.
MR	12.6-78.7	30.7	MR site

51

52